CAPITAL UNIVERSITY OF SCIENCE AND TECHNOLOGY, ISLAMABAD

Chitosan-based pH Responsive Hybrid Hydrogels for Drug Delivery Applications

by

Maria Kanwal

A thesis submitted in partial fulfillment for the degree of Master of Science

in the

Faculty of Health and Life Sciences
Department of Bioinformatics and Biosciences

2025

I DEDICATE THIS EFFORT & FRUIT OF MY THOUGHTS TO
HAZRAT JAHANGIR TAMIMI (R.A), DR. ATTA RASOOL,
MY PARENTS, LOVING HUSBAND,
&
MUHAMMAD SAADEH ANEES

CERTIFICATE OF APPROVAL

Chitosan-based pH Responsive Hybrid Hydrogels for Drug Delivery Applications

by

Maria Kanwal

(MBS233002)

THESIS EXAMINING COMMITTEE

S. No.	Examiner	Name	Organization
(a)	External Examiner	Dr. M. Zeeshan Bhatti	NUMS, Rawalpindi
(b)	Internal Examiner	Dr. Erum Dilshad	CUST, Islamabad
(c)	Supervisor	Dr. Muhammad Asad Anwar	CUST, Islamabad

Dr. Muhammad Asad Anwar
Thesis Supervisor
September, 2025

Dr. Syeda Marriam Bakhtiar
Head
Dept. of Bioinfo. & Biosciences
September, 2025

Dr. Sahar Fazal
Dean
Faculty of Health & Life Sciences
September, 2025

Author's Declaration

I, **Maria Kanwal** hereby state that my MS thesis titled "**Chitosan-based pH Responsive Hybrid Hydrogels for Drug Delivery Applications**" is my own work and has not been submitted previously by me for taking any degree from Capital University of Science and Technology, Islamabad or anywhere else in the country/abroad.

At any time if my statement is found to be incorrect even after my graduation, the University has the right to withdraw my MS Degree.

(Maria Kanwal)

Registration No: MBS233002

Plagiarism Undertaking

I solemnly declare that research work presented in this thesis titled "**Chitosan-based pH Responsive Hybrid Hydrogels for Drug Delivery Applications**" is solely my research work with no significant contribution from any other person. Small contribution/help wherever taken has been duly acknowledged and that complete thesis has been written by me.

I understand the zero tolerance policy of the HEC and Capital University of Science and Technology towards plagiarism. Therefore, I as an author of the above titled thesis declare that no portion of my thesis has been plagiarized and any material used as reference is properly referred/cited.

I undertake that if I am found guilty of any formal plagiarism in the above titled thesis even after award of MS Degree, the University reserves the right to withdraw/revoke my MS degree and that HEC and the University have the right to publish my name on the HEC/University website on which names of students are placed who submitted plagiarized work.

(Maria Kanwal)

Registration No: MBS233002

Acknowledgement

All praises to Almighty Allah who has given me the wisdom to identify the right path to successfully complete this research. All respects to the Holy Prophet (PBUH) for enlightening my conscience with the essence of faith in Allah, converging all His kindness and mercies upon me.

I would like to express my heartfelt gratitude to my supervisor Dr. Muhammad Asad Anwar (Assistant Professor, Department of Bioinformatics and Biosciences, CUST) for providing me the valuable opportunity to perform this research under his supervision. He has supervised the work with personal dedication, continuous efforts, support and guidance, which kept me motivated during my research.

I am beholden to Dr. Atta Rasool for extending prudent advices, sympathetic attitude, moral support, inspiring comments and strong motivation to address the problems encountered during my research work. My special thanks to my husband Dr. Muhammad Anees Ur Rehman Qureshi for his support, valuable advices and encouragement for the successful completion of this work.

Thanks to all.

(Maria Kanwal)

Abstract

Silver sulfadiazine (AgSD) belongs to the class of sulfonamide, a broad spectrum antibiotic. It is widely used for treatment of burn, infected and chronic wounds because of its degradation into Ag^{+1} and sulfadiazine. However, topically AgSD has limited bioavailability, less solubility and poor penetration. On the other hand, chitosan (CS) based hydrogels demonstrated lower stabilities and lesser drug loading efficacies. Consequently, in present work, we have prepared functionalized sepiolite (F-SEP) incorporated CS and poly(ethylene glycol) (PEG) hydrogels by solution casting technique for improved AgSD delivery and wound dressing applications. The fabricated hydrogels were characterized by Fourier transform infrared spectroscopy, X-ray diffraction, thermal gravimetric analysis and scanning electron microscopy that confirmed modifications in sepiolite (SEP), development of hydrogel interfaces and successful AgSD encapsulation. Hydrogels exhibited swelling capabilities as a function of F-SEP in distilled water that obeyed non-Fickian diffusion phenomenon. The higher swelling volumes were recorded at pH 2 and 7. Biodegradation test confirmed their highly degradable nature. F-SEP not only imparted higher swelling % in hydrogel matrices but also promoted AgSD encapsulation, antibacterial activity and thermal resilience. In 30 hours, 81.27% of the drug release was observed by using UV-visible spectrophotometer. AgSD release from DSAR-15 depicted best fit for Korsmeyer-Peppas model with regression cofficient 0.978. AgSD release from the gel matrix involved swelling as well as diffusion process. The biodegradable and pH responsive CS/PEG/F-SEP hydrogel platform could be a valuable choice for sustained delivery of AgSD and therapeutic payloads for development of efficient dressings for healing wounds. In future, these hydrogels could also be exploited for tissue engineering, bone regeneration, and slower release of fertilizers.

Contents

List of Figures

List of Tables

Abbreviations

AgSd	Silver sulfadiazine
Alg	Alginate
APTS	3-Aminopropyl(triethoxy)silane
CS	Chitosan
E. coli	*Escherichia coli*
EE	Encapsulation efficiency
FE-SEM	Field emission scanning electron microscope
F-SEP	Functionalized sepiolite
FTIR	Fourier transform infrared spectroscopy
GO	Graphene oxide
HEK-293	Human embryonic kidney cells-293
MTT	(3-(4,5-dimethylthiazol-2-yl)-2,5-diphenyltetrazolium bromide)
PBS	Phosphate buffer saline
PEG	Poly(ethylene glycol)
PVA	Poly(vinyl alcohol)
PVP	Poly(N-vinylpyrolidone)
ROS	Reactive oxygen species
SEP	Sepiolite
TGA	Thermal gravimetric analysis
XRD	X-ray diffraction

Chapter 1

Introduction

Despite of pharmaceutical advancements in 21^{st} century, preventing deaths from resistant bacterial infections, maintaining communal belief and low therapeutic indexes are currently existing challenges. Traditional drug delivery systems have severe cytotoxic effects on healthy cells. Therefore, pharmaceutical industries are encountering the concerns related to the product quality, safety, compliance and cost effectiveness. In the same linking manner, degradation of drug molecules due to enzymatic actions and hydrolysis are root causes of premature clearance and poor bioavailability. There are different approaches like enteric coatings, targeted delivery and pH sensitive release systems that are helpful in providing optimum bioavailability. In the case of locally administered drugs, more chances are there for drug molecules to enter into systemic route by diffusion leaving minimal drug at the affected site for a therapeutic response. In order to achieve the maximum therapeutic effect at the target sites for optimum results, drug must be administered in a targeted way which not only improve compliance but also produce desired therapeutic responses [1].

On the other hand, Ag sulfaidiazine (AgSD) is a broad spectrum, bacteriostatic antibiotic that belongs to the group of sulfonamides. It is used for the treatment of burn wounds and bacterial infections in different parts of the body like ears, brain and urinary tract. The chemical structure of AgSD is depicted in Figure 1.1. It is estimated that more than 75% of deaths in burn patients are due to the

multiple infections at wound sites [2]. In addition, according to a report published by Soedjana *et al.* 180,000 peoples are died only because of burn wounds annually [3]. Although, different strategies are opted to prevent infections at burn and wound sites but death rates are quite high. In this regard, AgSD is an excellent choice for wound healing and antimicrobial actions because of its degradation into sulfadiazine and $Ag^{+}4$ ions. Ag^{+} ions inhibit synthesis of triphosphates in bacteria and sulfadiazine prevents formation of folic acid in them. Both these factors not only disrupt DNA replication but also terminate bacterial reproductive processes [4].

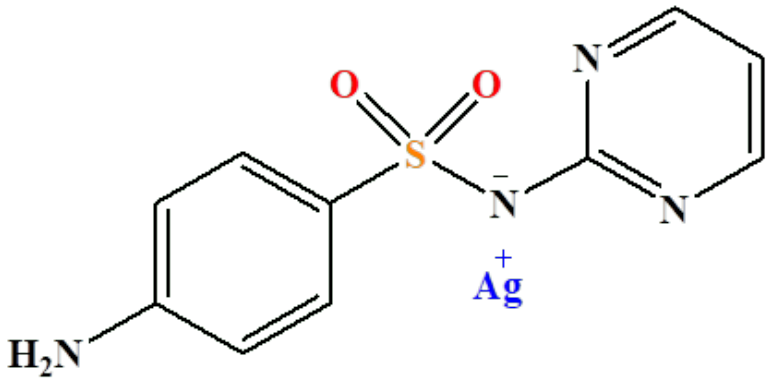

FIGURE 1.1: Structural representation of AgSD antibiotic [5].

The poor solubility, inflammation and limited penetration of AgSD are challenges in the effective delivery of this antibiotic. Consequently, controlled release systems and CS-based formulations are preferred to promote its solubility/penetration along with sustained release.

1.1 Hydrogels

Hydrogel-based carriers attracted considerable attention for drug delivery and wound healing purposes because of their hydrophilic, cross-linked and three - dimensional polymeric networks. These are made up of polymers, either natural, synthetic or semi-synthetic which absorbs and retains lot of water without dissolving in it [6]. Because of their porous, hydrophilic and water absorbing nature, these have properties similar to the living tissues and cells [7]. Synthesis of hydrogels

can be carried out by variety of methods such as co-polymerization, free radical polymerization, irradiation induced cross-linking, freeze thawing method, solution casting, graft copolymerization, sol gel method, polyelectrolyte complexation process, etc. However, initiators are prerequisite to begin polymeric interactions where monomers contain double bonds [8].

Conventional hydrogels exhibit poor drug loading/release for targeted administration of pharmaceutical cargos. To broaden the scope of hydrogels, it is imperative to design non-toxic hydrogel materials for biomedical application having superior weight bearing capacities and mechanical strengths coupled with improved drug adsorption/release.

As a wound dressing, hydrogels not only provide a moist environment that generate soothing and cooling effect at wound site but also absorb wound debris, softens necrotic tissues, promote cell migrations, accelerate re-epithelialization and prevent dressing stickiness [9–11].

In addition, hydrogel's swelling effectively respond to environmental stimuli like pH, ionic strength, electric field, enzyme, temperature, heat, pressure, sound, light, etc. which could be tuned, tailored and modified to deliver anti-infective agents at wound site [12].

1.2 Swelling Ability

The swelling action is a unique property of hydrogels in diverse solvents like water, pH, biological fluids and electrolytes enabling to exploit them in variety of fields namely biomedicine, soft robotics, agriculture, biology, industry, medical, bioseparations, environment, etc. [13]. The major steps involved in hydrogel swelling are depicted in Figure 1.2. Dehydrated and swollen forms of hydrogels are named as glassy and rubbery states, respectively. When water diffuses into hydrogel matrix, it relaxes bonds among polymeric moieties. Resultantly, hydrogel expands and changes from glassy into rubbery state [14].

1.3 Properties of Hydrogels

Hydrogels have brilliant swelling and elastic properties. Their shapes can be altered easily and are soft in their physical appearance. In addition, these efficiently respond to temperature, pressures, magnetic field, electric field, ionic strength and pH. Hydrogels are also biocompatible and immuno-compatible materials because of their resemblance to living tissues along with no inflammatory responses. Importantly, these are degradable and non-toxic that enable them an agent of choice for wound dressings, tissue engineering and other medico-biological applications [15]. Swelling capabilities and porous nature enable hydrogels one of the excellent medium for the delivery of drugs, therapeutic agents and biological compounds.

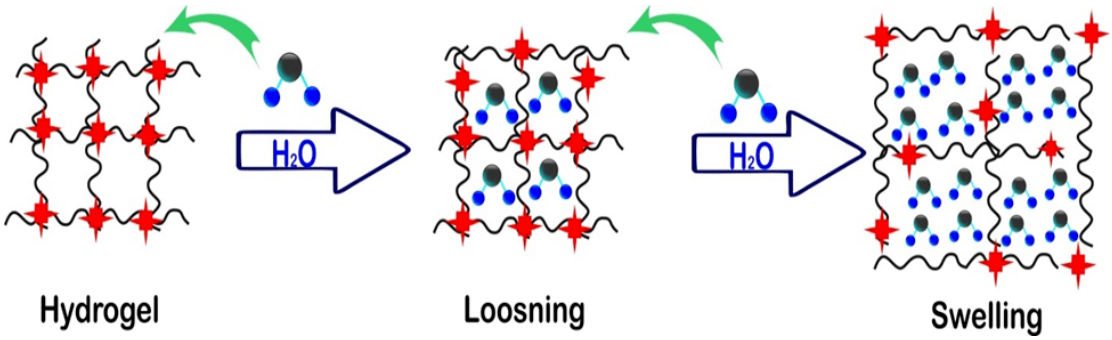

FIGURE 1.2: Three steps in hydrogel swelling [16].

1.4 Classification of Hydrogels

Hydrogels can be classified on the basis of their physical properties, composition, preparatory methods, kind of swelling, origin and type of cross-linking. Hydrophobic association, crystallization, chain aggregation, hydrogen bonding and polymer chain complexion are the physical processes to achieve cross-linking in hydrogel frameworks. On the other hand, chemical cross-linking is a chemical process that is exploited to develop covalent linkages to acquire chemical hydrogels. Double-network hydrogel is another category of physicochemical hydrogel which comprises the properties of both physical and chemical hydrogels [17]. Likewise, on the basis of charge hydrogels are divided into cationic, anionic, non-ionic and zwitterionic

hydrogels. Polymeric origin is another benchmark in order to categorize the hydrogels. Hydrogels made up of natural, synthetic and natural-synthetic polymers are regarded as natural, synthetic and hybrid hydrogels, respectively.

On the basis of response hydrogels are divided into numerous types such as pH sensitive, temperature sensitive, light sensitive, enzyme sensitive, pressure sensitive hydrogels, etc.

1.5 pH Sensitive Hydrogels

Hydrogels containing polar and charged groups represents swelling regulated by the pH of medium. This pH dependent swelling actions are dependent on ionic charge, hydrophilicity, pH of medium and pK_a of ionizable groups. pH and polymeric functional groups are crucial factors imparting pH responsive behaviors in hydrogels. Cationic hydrogels swell in acidic pH and vice versa [18].

Hydrogels depicting good swelling performance above pH 7 are exploited to facilitate targeted release of medicines in intestine around 7.4 pH [19].

Chitosan (CS), collagen, alginate (Alg), hyaluronic acid, carrageenan, agarose, cellulose, polyphenols, xanthan, pectin, starch, agar, gelatin, chitin, gaur gum and fibrin are some important biopolymers for fabrication of pH responsive hydrogels [20]. In the same way, poly(ethylene glycol) (PEG), poly(N-isopropylacrylamide), poly (N-vinylpyrrolidone) (PVP), poly(ethylene oxide), poly (acrylic acid), poly (urethane), poly (acrylamide), poly (methyl methacrylate), poly (caprolactone), and poly (vinyl alcohol) (PVA) are synthetic polymers to make pH receptive hydrogels [21].

Thus, pH sensitive swelling capabilities of hydrogels are tuned for targeted and sustained release of drugs, agro-chemicals and nutrients. Table 1.1 reflects normal pH of some human organs and fluids.

1.6 Materials in Hydrogel Synthesis

Hydrogels are unique and versatile materials which can be synthesized by variety of natural and synthetic polymers. Depending upon type of applications the reinforcement materials, nanoparticles, dendrimers, clays and cross-linkers are incorporated in hydrogel systems to acquire desired properties. For instance, polyamidoamine dendrimer, graphene oxide (GO) and sepiolite (SEP) are added to promote drug release, enhance mechanical properties and improve drug dissolution in hydrogels, correspondingly.

TABLE 1.1: The pH of human organs/fluids.

Organ/fluid	pH Range	References
Blood	7.35-7.45	
Stomach	2.0	
Colon	7.0-7.5	[22]
Duodenum	5.0-8.0	
Jejunum	6.0-7.0	[23]
Ileum	7.0	
Rectum	4.0-5.0	
Vagina	4.0-5.0	[24]
Cecum	6.4	[25]
Saliva	6.7-7.3	[26]

1.6.1 Biopolymers

Biopolymeric hydrogels are prepared from natural polymers only. These polymers are widely available, abundant, affordable, non-toxic, biodegradable, and have attractive biological features [27]. In Figure 1.3, chemical structures of some biopolymers are represented which are used in fabrication of hydrogels. Polysaccharides, nucleic acids, polyamides, polyisoprenoids, polythioesters, polyphenols, organic and inorganic polyesters are different classes of natural polymers. However, bio-polysaccharides are unique family of naturally available polymers that are rich in structural as well as functional diversity [28]. These are also useful as renewable, modifiable and inexpensive biomaterials because of their exceptional

bioactive, non-immunogenic, biocompatible, non-carcinogenic and harmless nature.

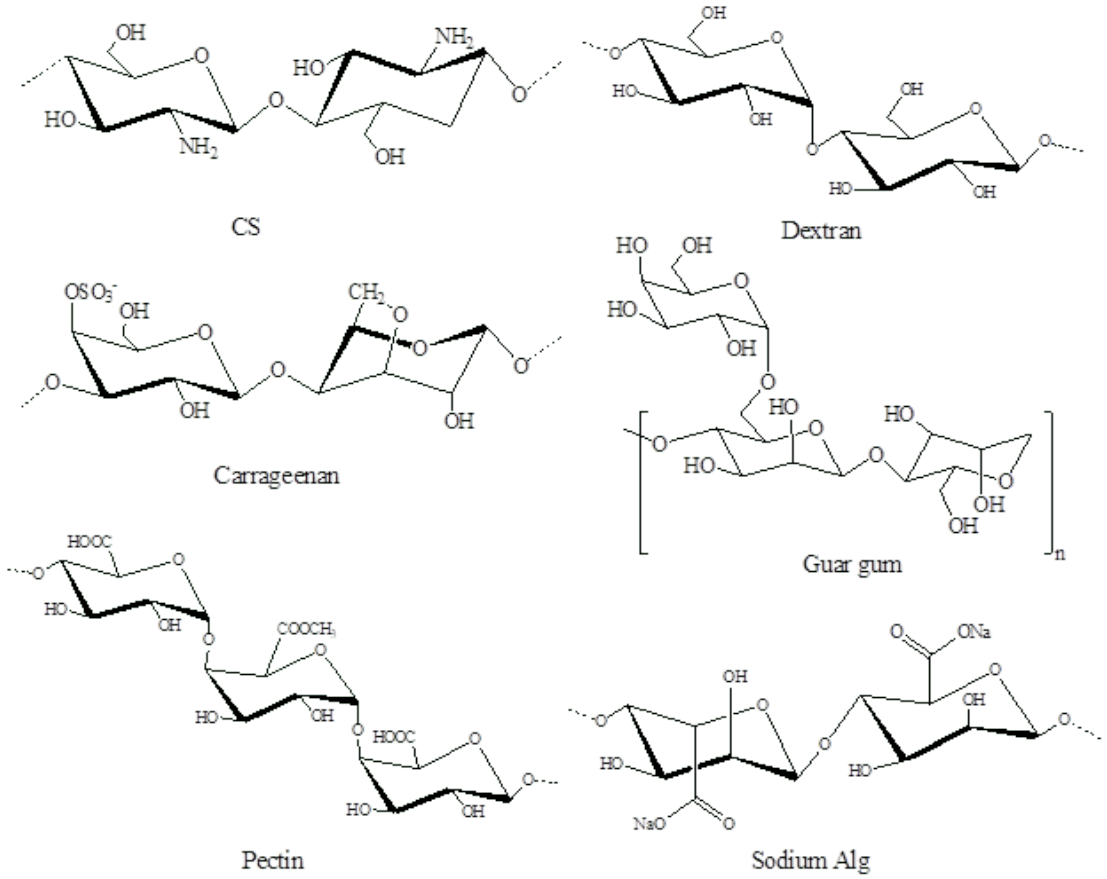

FIGURE 1.3: Structural depiction of biopolymers along with their pendant groups [29].

CS is prepared by replacement of acetamido group in chitin with NH2 group as shown in Figure 1.4. It is nontoxic, biocompatible and biodegradable biopolymer [30]. Its hydrophilic, adhesive and modifiable nature makes it an excellent choice in wound healing and drug delivery applications. Although, CS films are poor in their mechanical properties but, natural-synthetic polymeric combination, modification of amino and hydroxyl groups and introduction of filler are common approaches to acquire desired mechanical properties in its films and gels [31]. The key functional groups involved in the synthesis of CS-based hydrogels are hydroxyl and amino groups that could be modified for desired properties like swelling, gelation, degradation and hydration [32]. For instance, Islam *et al.* reported CS/PVA hydrogels chemically cross-linked by tetra ethoxy-orthosilicate. The hydrogel blends

displayed maximum swelling capacity at pH 7. Consequently, the reported system was an ideal choice for oral administration of medicines, therapeutic cargos, nutrients and enzymes [33].

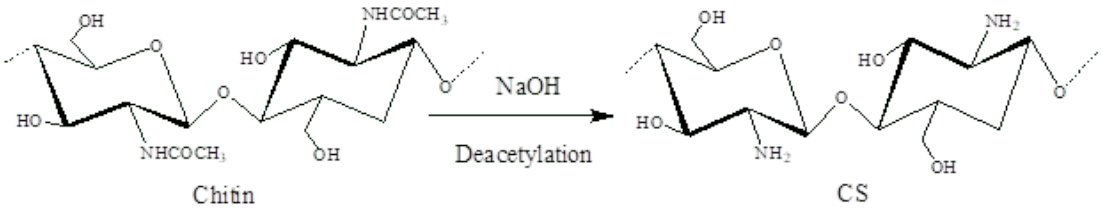

FIGURE 1.4: Chitin de-acetylation to prepare CS [34].

The hydrogels composed of pure CS biopolymer have poor strength which limits their utilization in drug delivery. Subsequently, hybrid hydrogels are prepared by mixing synthetic and biopolymers [35].

Synthetic polymers improve strength and modify physicochemical properties in hydrogel matrices [36]. PVA, PVP, PEG, poly(acrylic acid), etc. are synthetic polymers extensively exploited for synthesis of hydrogels for wound healing, tissue engineering, and drug delivery.

1.6.2 Synthetic Polymers

Synthetic polymers are selected in medico-biological industry because of their economical manufacturing, easier processing, degradation, flexibility in modifications and higher mechanical performance [37]. Thus, in order to get a collective advantage and better physicochemical properties, cross-linking biopolymers with synthetic polymers is useful to acquire desired structural features in hydrogels [38].

PEG, PVA, PVP, poly (urethane), poly (caprlactone), etc. are synthetic polymers widely utilized for fabrication of hydrogels in variety of biomedical applications such as wound healing, tissue engineering, wound dressing, regenerative medicines and drug delivery [39]. Figure 1.5, reflects important synthetic polymers exploited to produce hybrid hydrogels for drug delivery and medico-biological applications.

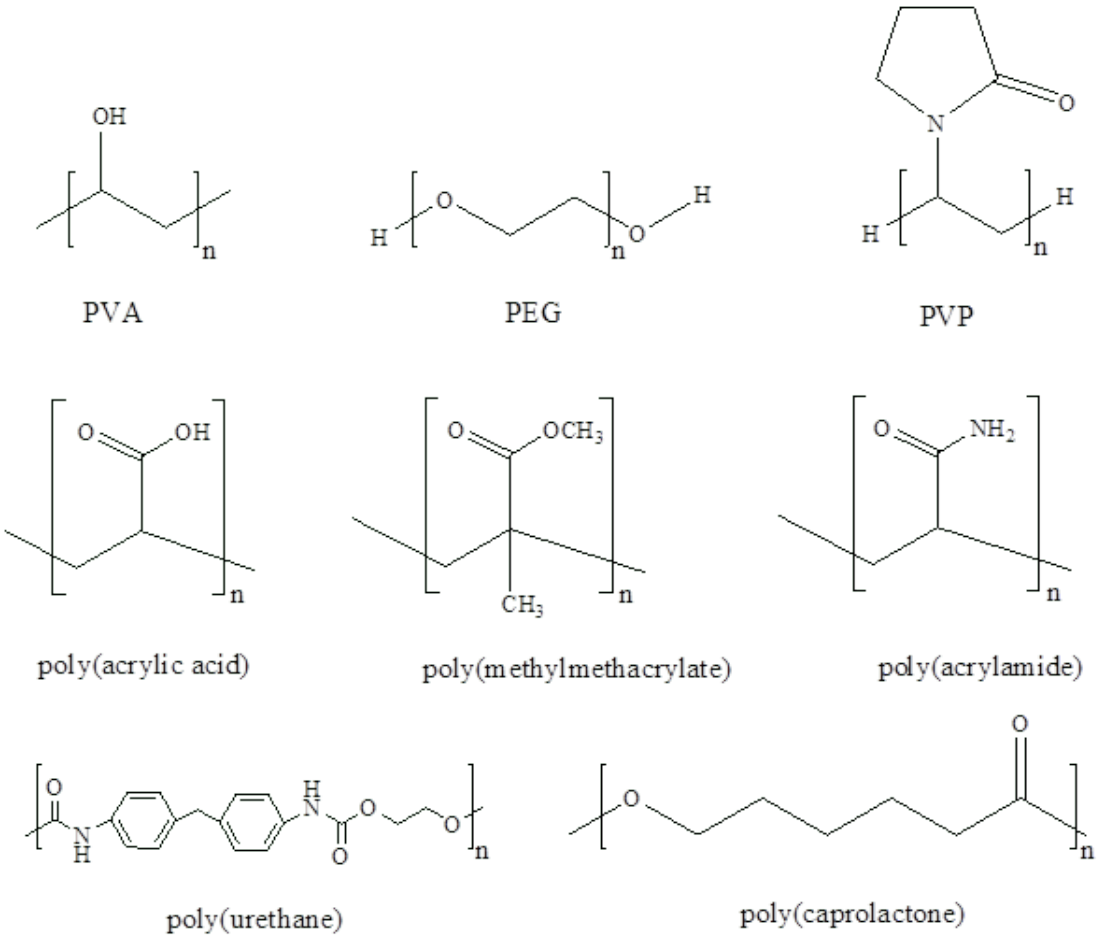

FIGURE 1.5: Some synthetic polymers exploited to modify hydrogel properties [40].

PEG is hydrophilic, tasteless, highly water soluble, inert and biocompatible polymer which is exploited in fabrication of three-dimensional hydrogels for cartilage regeneration, gene therapy, drug delivery, colonoscopy, bone repair, coating implants, tissue engineering, nerve regeneration and wound dressing applications [41–44]. Its inherent two hydroxyl groups could be transformed into azide, methoxyl, carboxyl, acrylate, amine, thiol and sulfane functionalities. On other hand, it is already used in surgical scrubs, tablets, medical equipment and eye ointments [45]. Rasool *et al.* inspected the impact of mutable PEG molecular mass on carrageenan/Alg-based hybrid hydrogel cross-linked by 3 - aminopropyl (triethoxy) silane (APTS) for controlled lidocaine release. The increase in PEG molecular mass inversely effected antibacterial performances [46].

1.6.3 Role of Filler

In drug delivery, hydrogel exhibit poor drug loading/release [47]. Therefore, fillers are used which enhance stability, induce mechanical strength and improve drug loading/release by providing high surface area. In addition, fillers also impart new physical and chemical properties in hydrogel systems [48]. Recently, researchers reported that addition of SEP clay in hydrogel matrix not only improves drug loading/release but also remarkably enhance mechanical properties [49].

SEP is a soft, porous, white, fibrous, needle-like, hydrous and lightweight clay of magnesium silicate with chemical formula $Mg_4SiO_{15}(OH)_2.6H_2O$. Stabilization of SEP can be improved by using poly electrolytes and mechanical dispersion technique [50]. It is incorporated as filler in hydrogels not only to enhance surface area but also to improve drug loading and release. SEP is expected to improve dissolution of poorly soluble drugs in order to enhance their bioavailability [51].

1.6.4 Cross-linkers

Cross-linkers are used to chemically bind the different components of hydrogels. In previous studies, hydrogels were mostly made by using cytotoxic cross-linkers like glutaraldehyde, genipin, borate, epichlorohydrin, etc. [52]. Food and drug administration approved silane-based cross-linkers which demonstrated better results in human systems owing to their non-toxic, and biodegradable nature. Silane-based cross-linkers generate binding among natural/synthetic polymers and fillers by their amine, amide, carboxyl and hydroxyl functional groups [53].

1.7 Problem Statement

Much attention has been given to develop hydrogels for drug delivery systems. However, traditional hydrogels are prepared by toxic cross-linkers and also demonstrated lower drug loading/release ability. Therefore, it is imperious to design pH

sensitive, biocompatible and inexpensive hybrid hydrogels by using functionalized SEP (F-SEP) and silane-based cross-linkers for drug delivery applications.

1.8 Scope of Study

Conventional drug delivery systems have shown complete and rapid release of drugs that has severe physicochemical effects on normal cells. Consequently, researchers have shown great interest to design biopolymeric hybrid hydrogels for drug delivery and wound dressings.

However, development of more efficient and non- toxic hydrogel dressing capable for controlled release of drug is a major challenge.

In present work, the fabricated hydrogels will inherit biocompatibility and hydrogel formation capability from CS biopolymer.

On the other hand, PEG breeds mechanical strength in hydrogels. SEP is modified/functionalized with APTS cross-linker and denoted as F-SEP.

The F-SEP not only cross-links CS and PEG but also improve AgSD loading/release by providing higher surface area to volume ratio and greater dissolution/penetration. Moreover, it is a novel, easy, cost effective and non-toxic hydrogel platform as compared to previously reported methods incorporated with toxic cross-linking agents like glutaraldehyde, borate, epichlorhydrine, etc.

1.9 Hypothesis

Functionalized sepiolite integrated chitosan/poly(ethylene glycol) hydrogels will demonstrate pH sensitive, cytocompatible, biodegradable and sustained release of therapeutics for drug delivery applications.

1.10 Aim

Development of functionalized sepiolite reinforced inexpensive, cytocompatible, biodegradable and pH responsive chitosan/poly(ethylene glycol) hydrogel platform for sustained drug release applications.

1.11 Objectives

1. To synthesize efficient hydrogels for drug delivery system by combining chitosan biopolymer and poly(ethylene glycol) synthetic polymer using functionalized sepiolite.

2. To determine swelling capabilities of the hydrogels in distilled water, buffer and non-buffer solutions to confirm their pH sensitive behaviors.

3. To investigate in-vitro drug release from drug loaded hydrogels through UV-visible spectroscopy.

4. To determine biodegradation, cell viability and encapsulation efficacy in order to exploit hydrogels for in-vivo drug delivery and wound dressings systems.

Chapter 2

Literature Review

This section spotlights review of literature related to the CS-based hydrogels, their applications and recent developments.

2.1 CS-based Hydrogels

The blends of CS with other natural/synthetic polymers expanded its utilization in numerous fields. The hydrogel forming capability of CS is an important development. This advancement led researcher working in polymeric and biomedical sector to realize hydrogel significance in biological systems. CS contains amino and hydroxyl groups which can be modified and converted into other groups in order to mend hydrogel properties [54]. The blends of CS with other natural and synthetic polymers have attained considerable attention in recent years for different medico-biological applications [55]. In hydrogel fabrication, the terminal hydroxyl groups existent in PEG allow its cross-linking. This is how, it modifies hydrogel architecture and upgrades their tensile properties.

Biocompatible, biodegradable hydrogels have been designed by using biopolymers that are susceptible to enzymatic degradation or using synthetic polymers that possess hydrolysable moieties. Of these, hydrogels CS have received a great deal of attention due to its well reported biocompatibility, low toxicity and degradability

by human enzymes [56]. When CS aqueous solutions are combined with other components like polyol salts and polyhydroxy polymers then, temperature sensitive CS hydrogels are obtained. These hydrogels are fluid at room temperature and become a transparent gel at temperatures above 35 ^{o}C. Therefore, these can be opted as injectable materials for drug delivery applications [57].

Rasool *et al.* reported CS/PVP hydrogels cross-linked by APTS that exhibited maximum swelling activity at pH 2. The hydrogel blends also demonstrated controlled cefixime release (81.6%) up to 12 hours. Author concluded that, this could be useful model platform for delivery of drugs in acidic environment. The same research group also fabricated the CS/PVP/poly(acrylic acid) formulation loaded with AgSD for wound healing applications. Poassium persulfate initiator was used to chemically bound hydrogel ingredients. Hydrogels demonstrated maximum swelling actions at pH 8. Moreover, 91.2% sulfafiazine was released in phosphate buffer saline solution (PBS) in 1 hour [58].

In the same liking manner, Qureshi *et al.* investigated effect of variable quantity of GO on CS/PVP/polyamidoamine (PAMA) dendrimeric hydrogels. It was inferred that increase in GO decreased the swelling capacities and upgraded the thermal resilience and degradation behaviors of CS/PVP/PAMA/GO hydrogels. In 4 hours, 83.7% of cephradine was released in sustained manner. This platform represented maximum swelling and release of cephradine antibiotic at basic pH (8.0). Therefore, this could be useful for delivery of drugs in intestine [59]. Further, the research group also prepared similar composition of CS/PVA/GO by mutable amount of PAMA. The highest swelling performances were recorded at pH 4. The resulting hydrogels reflected 85% of cefixime release in 8.5 hours in simulated gastric fluid. The reported platform seems to be promising and reliable for medico-biological applications [60]. Likewise, Naz *et al.* reported CS-based nanofibers that reflected 90% of cephradine release in 2 hours and 40 minutes [61].

Sorasitthiyanukarn *et al.* synthesized CS/Alg hydrogels system loaded with curcumin diglutaric acid nanoparticles for oral delivery. The fabricated hydrogel system displayed good stability in gastrointestinal environment coupled with excellent cellular uptake of curcumin diglutaric acid as compared to its direct use.

The release of curcumin diglutaric acid from hydrogels followed Weibull kinetics. Authors stated that CS/Alg loaded with curcumin diglutaric acid nanoparticles could be a model platform which can improve its anticancer efficiency [62].

Lejardi *et al.* modified PVA with glycolic acid and then blended it with CS to produce hydrogels. The pH of blending mixture was maintained at 6.8 at ambient temperature. It was deduced that plasticity and flexibility of hydrogel material was considerably improved by the increase in the amount of afore-mentioned modified PVA. Author claimed these hydrogel composites could be useful as injectable for biomedical engineering [63]. Laura *et al.* formed semi-interpenetrating hydrogel materials made of CS/agarose cross-linked by dextrin. Author also examined the role of hydrogel composition and extent of dextrin oxidation on development of hydrogel frameworks. The development of networks in hydrogel is governed by dextrin degree of oxidation. Moreover, slight amount of agarose directly effects the formation of frameworks. The reported hydrogels are seemed to be appropriate for three-dimensional printing, tissue engineering and wound dressing purposes [64]. In the same liking manner, Zhang *et al.* formulated pH and thermal responsive carboxymethyl CS /poly (N - isopropylacrylamide) - glycidyl methacrylate hybrid injectable materials by ultraviolet radiations for local administration of drugs [65].

Islam *et al.* fabricated CS/PVA hydrogels chemical cross-linked by silane cross-linker namely tetra-ethoxy ortho-silicate. The changes in the PVA content in CS/PVA hydrogels inversely influenced the swelling in hydrogel. CS/PVA hydrogels have also demonstrated pH dependent swelling. Hydrogels showed highest swelling volumes at pH 7, while lower swelling volumes were calculated in acidic and basic media. This characteristic pH sensitive swelling could be explored for oral administration of therapeutic payloads [66].

Fujun *et al.* developed bactericidal CS/starch hydrogel membranes. The flexibility in the membranes was established by the addition of glycerin as plasticizing agent. In this way, the elongation at break were enhanced that might be due to the association of -OH group of starch and -NH2 moiety of CS. These hydrogel materials represented excellent antibacterial action against Escherichia coli (E.

coli) [67]. Archana *et al.* synthesized wound dressing by loading TiO_2 nanoparticles on CS/pectin to determine wound healing, antimicrobial and biocompatible property. The photo sensitive responses of TiO_2 enable its use as biosensors for medical uses. CS can be simply processed into gels, membranes, films, scaffolds, nanofibers, beads and nanoparticles which can be used for wound healing purposes [68].

2.2 Applications of Hydrogels

Hydrogels are useful, diverse and flexible in their applications in different fields like biomedicine, water purification, dyes adsorption, controlled release of agrochemicals, food preservation, water proofing, diaper industry, permeable membranes, biosensors, soil improvement, wastewater treatment, growth in nurseries, hygiene products, etc. [69–71]. In biomedical industry these are extensively used in wound care, contact lens, cancer treatments, ocular ointments, dental care and regenerative medicines. In tissue engineering, hydrogels are employed as drug carrier, filler, cell support materials and also aid in ideal tissue development [72]. In Figure 2.1, applications of hydrogels in biomedical sector are summarized.

However, majority applications of hydrogels are focused on drug delivery. Intelligent hydrogels in the drug delivery systems smartly respond to the physiological needs, sense changes and then adjust the drug release pattern accordingly. Smart hydrogels also adjust the drug delivery profiles by self-regulated or pulsed mechanisms [73]. Researchers have extensively concentrated on preparation and investigation of hydrogels built by various polymers for drug delivery purposes [74]. Hydrogels that swell and contract in response to external pH possess potential application in the site-specific delivery of drugs to specific regions of gastrointestinal tract [75]. In Table 2.1, advatages and disadvantages of CS-based hydrgels are vetted.

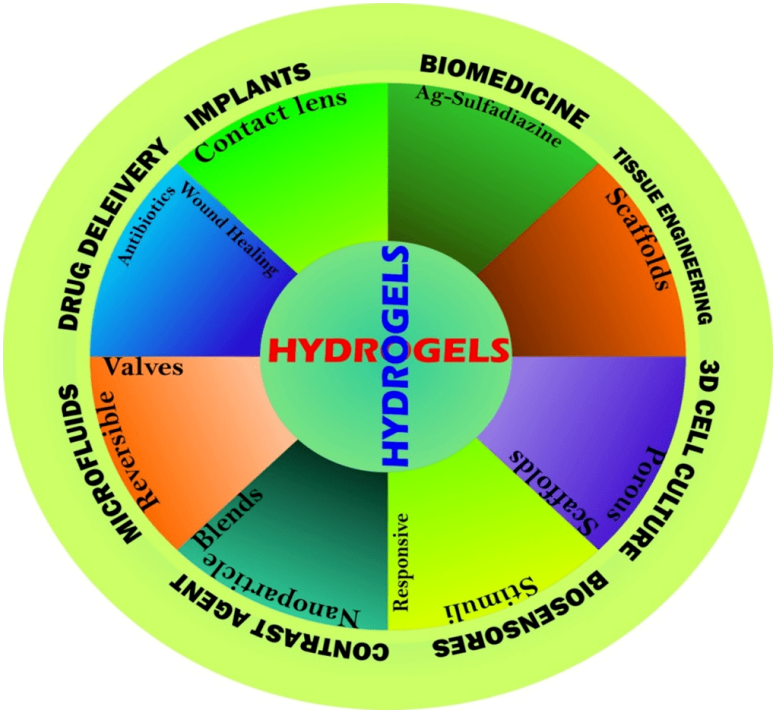

FIGURE 2.1: Hydrogels applications in biomedical engineering.

TABLE 2.1: CS in hydrogel applications

Advantages	**Disadvantage**
• Antimicrobial	• Cross-linking in CS may affect its intrinsic properties
• Antibacterial	
• Anti-oxidant	
• Non-toxic	
• Porous in structure	
• Biocompatible	
• Softens the skin	
• Biodegradable	
• Modifiable	
• Bioactive	
• Abundant	
• Inexpensive	

Transplantation is not feasible for organ replacement because of limited donors. Therefore, tissue engineering and three-dimensional bioprinting are the modern techniques that are used to repair and regenerate damaged and even lost tissues. The structural similarity of CS with glucosaminoglycans enable it an excellent

choice for tissue engineering [76]. The major problem with CS is its poor strength and brittle films. Consequently, its scaffolds are prepared by the combination of natural and synthetic polymers with aid of chemical cross-linker. In addition, the flexibility of scaffolds is achieved by the addition of plasticizer like glycerin [77]. For example, Wang and his coworkers incorporated cellulose acetate, poly(acronitrile) nanofibers and SiO2 nanofibers in CS matrix that resulted in enhanced mechanical performance [78].

Recently, Qureshi *et al.* reported poly(amididoamine)/carrageenan/Na-Alg/PVA hydrogels cross-linked by changing the concentration of 3 - aminopropyl (diethoxy) methyl silane. Hydrogels revealed excellent cell viabilities against DF-1 fibroblasts cells and proven their biodegradable and biocompatible nature. In 13.5 hours, 81.25 and 77.23% of methotrexate was released at pH 7.4 (blood pH) and 5.3 (tumor pH) in PBS by super case II mechanism and best fitted to Zero order and Korsmeyer-Peppas model. The synthesized Alg-based dendrimeric hydrogel platform could be effective for delivery of anti-cancerous compounds [79].

Diabetes and diabetic wounds are most burning challenge in present world in which not only blood glucose level rises from optimum level but also causes variety of microbial infections and inflammations on wound site. Currently, in practice anti-diabetic treatments have several limitations related to the bioavailability, side effects, dosage and prolonged action. Thus, Na-Alg and CS are promising candidates to solve these problems by efficient transport of anti-diabetic medicines [80]. Similarly, Mor and coworkers reported Alg modified guanidine derivative followed by coating of ZnO for bactericidal activity and precise release of curcumin. The reported platform demonstrated excellent antibacterial activity against both gram-positive and gram-negative bacteria. Author concluded that this platform could be ideal for development of wound dressings for diabetic wounds using Na-Alg/guanidine/ZnO nanoparticles [81].

There are numerous research reports for development of oral and gastrointestinal delivery platforms by exploring bio-adhesive, biocompatible, muco-adhesive and non-hazardous nature of Alg and CS to make tablets. Glycoproteins in gastrointestinal tract interact with CS which increases the time period of the CS-based

compounds in alimentary canal. Resultantly, the bioavailability of the loaded drug is enhanced [82]. Overall biomedical applications of CS-based hydrogels are summarized in Figure 2.2.

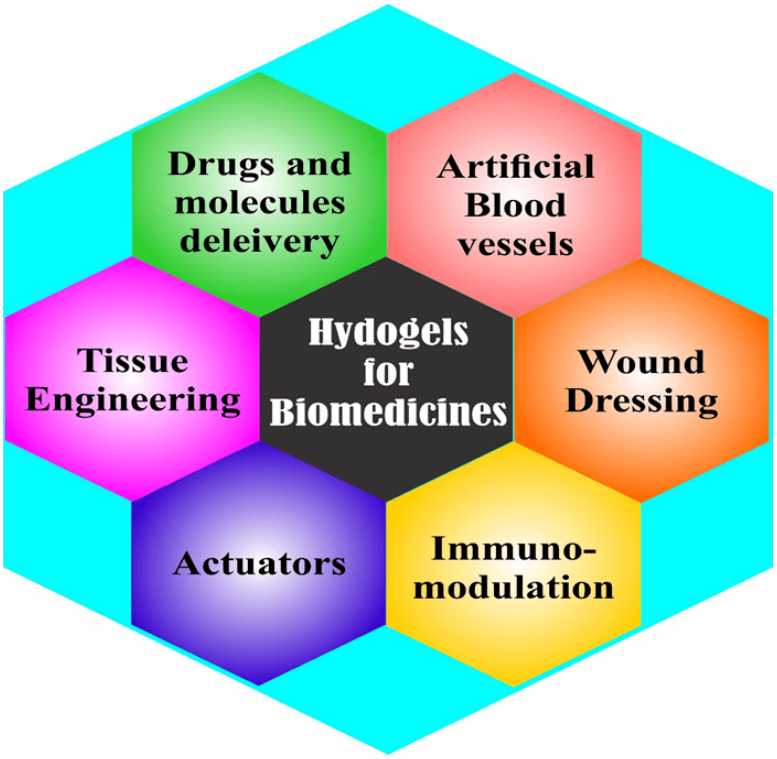

FIGURE 2.2: CS-based hydrogels for biomedical applications.

Adsorption is a cost-effective method for treatment of polluted waters. Now days, a cost effective and environment friendly hydrogel adsorbents are used. Hydrogels are capable to remove the pollutants and metal ions from the contaminated water [83]. CS-based hydrogels beads also provide more active binding sites for metal ions. Modified and cross-linked CS and its composites were also investigated as sorbents for removing copper (Cu^{2+}) and lead (Pb^{2+}) from aqueous solutions. These hydrogels have a high affinity for pollutants, such as heavy metals, organic contaminants and microorganisms, allowing them to effectively remove these substances from water sources [84].

2.3 CS-based Wound Dressings

CS-based wound dressings are reliable choice for curing wounds because, it effectively prevent entry of pathogens in the body. It also promotes RBC aggregation and platelets adhesion. Consequently, CS-based hydrogel dressings are preferred in burn, infection, diabetic and surgical wounds owing to their soft texture, safety, degradation and bio-adhesion.

2.3.1 Stages in Wound Healing Process

Wound management is a major clinical concern because of the complex process involved in healing process. Wound healing is a very complex, overlapped, regulated, multi-step and highly coordinated process. In this process variety of hormones, metallic ions, cytokines and cells are involved for repairmen of injured tissue. There are four steps involved in healing wounds namely, hemostasis, inflammation, proliferation and remodeling.

In hemostasis, blood vessels are damaged therefore, thrombin stops bleeding. Moreover, tissue factor initiate platelets activation followed by aggregation [85]. In the second inflammatory step, damaged cells release chemokines in order to appeal neutrophils and macrophages at the site of injury. The major role of neutrophil at injury site is to treat wound by their phagocytic and bactericidal actions that ultimately remove necrotic tissues as well as bacteria [86]. Macrophages also provide variety of growth factors necessary for the regulation of angiogenesis and remodeling [87]. In proliferation, critical events of wound repair take place including formation of granulated tissues, collagen formation, angiogenesis, epithelialization and transformation of fibroblasts into myofibroblasts [88]. The final step of wound repair process is remodeling in which collagen type-III is replaced by collagen type-I that breed toughness in the tissues to acquire pre-wound shape.

2.3.2 CS-based Hydrogels for Healing Skin Wounds

CS stands out as a promising biopolymer for the fabrication of dressings to cure skin wounds. This is because of its inherited extraordinary properties. For instance, CS hydrogels possess well reported antimicrobial activity to rupture the bacterial and fungal membranes [89]. In the same way, these hydrogels displayed self-healing capabilities along with stimuli responsive nature dependent upon pH, temperature, ionic strength, light, etc. Likewise, anti-oxidant property of CS hydrogels is effective to reduce reactive oxygen species (ROS) which is the main reason in chronic wounds.

In addition, positive charge in CS binds to the negative groups of cell membrane that enable CS- based hydrogels a highly effective hemostatic agent to stop bleeding, enhance aggregation and platelet adhesion. The above-mentioned properties of CS hydrogels motivated researchers to exploit them in skin wound dressings.

The high ROS in burn wound accompanied with pain, infections and fluid losses are the major factors leads to the chronic inflammation. Therefore, carboxymethly CS loaded with curcumin is reported by the Yang *et al.* for burn wounds to reduce ROS. Authors used ROS sensitive cross-linker during the synthesis.

Carboxymethly CS and curcumin accelerate burn wound healing. Moreover, by the passage of time curcumin also released from hydrogel dressing and provide further therapeutic effect by its anti-oxidant and anti-inflammatory activity [90]. Table 2.2 provides a brief summary of applications of CS-based hydrogel dressing for healing skin wounds.

Post-surgical infection and bleeding are the major causes of deaths. Therefore, biocompatible materials with multiple, antimicrobial, anti-oxidant, hemostatic activities are ideal. In this regard, CS hydrogels are hemo-compatible, cell friendly, inexpensive and flexible for the treatment of surgical wounds.

Geng *et al.* reported CS-based hydrogel incorporated with cynomolgus extract that demonstrated exceptional hemostatic ability in hemorrhagic liver *in-vivo*

model [91]. Tan *et al.* also used quaternized CS dressing with exceptional adhesion, water absorption, RBCs and platelet adhesion coupled with antimicrobial action [92].

In order to cure infected wounds, Bai *et al.* designed quaternary CS/hyaluronic acid/galic acid dressing. The resulting dressing demonstrated the excellent adhesion, drug release, degradation and hemostatic behavior. When the dressing was loaded with mupirocin, it aided in cell migration and enhanced anti-oxidant actions. In addition, this dressing effectively inhibited the factors causing inflammatory responses in wounds [93].

TABLE 2.2: CS-based hydrogels for the treatment of different kinds of wounds.

Hydrogel Dressings	**Application**	Reference
CS/poloxamer/hyaluronic acid	Burn wound	[94]
Collagen/CS	Burn wound grade III	[95]
CS/poly(urethane)/minocycline	Burn wound	[96]
CS/honey/gelatin	Burn wound grade II	[97]
CS/gelatin/sponge	Surgical wound	[98]
CS/sulphonamide	Surgical wound	[99]
CS/Ag nanoparticles	Surgical wound	[100]
Lipoic acid modified CS	Infected wound	[101]
Cefuroxime/CS	Infected wound	[102]
CS/PVA/mupirocin/CeO_2 nanoparticles	Infected wound	[103]
CS acetate	Infected wound	[104]
CS/PEG/methacrylate/ciprofloxacin	Infected wound	[105]
CS/acrylic acid/Ag nanoparticles	Diabetic wound	[106]
CS/PVA nanofiber	Diabetic wound	[107]
CS/streptozotocin	Diabetic wound	[108]
CS/microsphere/activated carbon	Chronic wound	[109]
CS/CeO2/vancomycin	Chronic wound	[110]

Chapter 3

Material and Methods

3.1 Chemicals and Reagents

CS (Mw: 190-310 kDa, viscosity > 200 cP, 75% deacetylation and bulk density 0.15-0.30 g/cm^3). PEG (Mw: 8000 g/mol, powder, 99% pure), SEP clay powder (Magnesium13%), APTS (Mw: 221.37 g/mol, faint yellow, 98% pure), sodium hydroxide (Mw: 40 g/mol) and calcium chloride (Mw: 110.99 g/mol, anhydrous), hydrochloric acid (Mw: 36.46 g/mol) and proteinase-K (Mw: 29kDa were procured from Sigma Aldrich. AgSD drug (357.14 g/mol, 99% pure) was purchased from a local company Henzils Pharma, Lahore, Pakistan. Finally, ethanol (Mw: 46.06 g/mol), Acetic acid (Mw: 60.5 g/mol, 99%), sodium chloride (Mw: 58.5 g/mol) and potassium chloride (Mw: 74.55 g/mol) were brought into use from Daejung. Beside afore-mentioned chemicals distilled water was used for solution preparations.

3.2 SEP Clay Modification

In 50 mL ethyl alcohol, 5g of SEP clay was added followed by the stirring for 2 hours at 80 ^{o}C. In subsequent step, 5 mL of APTS was poured in afore-mentioned

mixture and agitated for 24 hours. After that, the F-SEP (functionalized SEP) was thoroughly washed with deionized water

3.3 Hydrogel Preparation

Solution casting technique was used for synthesis of F-SEP incorporated CS/PEG hydrogels because of low temperature synthesis and flexibility in addition of filler [111]. In the first step CS (0.5g) was dissolved in 50 mL of 2% acetic acid. On the other hand, PEG (0.5g) was dissolved in 30 mL distilled water. In the second step, both above-prepared solutions were assorted under constant agitation at 70 ^{o}C for 2 hours to acquire a homogenous solution. In the third step, F-SEP (5, 10, 15 and 20 mg) was sonicated in 10 mL of deionized water up to 30 minutes and then transferred to blending mixture followed by incessant stirring for 3 hours. Finally, solutions were transferred in polystyrene petri plates to dry at room temperature to acquire dry hydrogels. The entire procedure for hydrogel fabrication was performed at 70 ^{o}C under persistent agitation. Hydrogel formulations were coded as SAR(cont), SAR-5, SAR-10, SAR-15 and SAR-20. The composition of each hydrogel film is provided in the Table 3.1.

TABLE 3.1: The composition of CS/PEG/F-SEP hydrogels.

Hydrogels	**CS (g)**	**PEG (g)**	**F-SEP (mg)**	**AgSD (mg)**
SAR(cont)	0.5	0.5	0	-
SAR-5	0.5	0.5	5	-
SAR-10	0.5	0.5	10	-
SAR-15	0.5	0.5	15	-
SAR-20	0.5	0.5	20	-
DSAR-15	0.5	0.5	15	100

3.4 Hydrogel Characterization

Following material characterization techniques were used for the characterization of hydrogels reported in present study;

3.4.1 Fourier Transform Infrared Spectroscopy (FTIR)

FTIR provides information about presence of different functional group in organic, inorganic and polymeric samples. It also identifies chemical bonding in molecules and produces infrared absorption spectrum. The spectrum creates a sketch regarding sample, a characteristic molecular fingerprint which can be utilized to screen and scan samples of numerous constituents. The development of hydrogel interfaces, binding/cross-linking, drug loading and existence of corresponding functional groups was confirmed by FTIR [112]. The dried hydrogels were subjected to the instrument under vacuum at a scan range of 400-4000 cm^{-1}.

3.4.2 Thermo Gravimetric Analysis (TGA)

In TGA physicochemical changes in mass of the sample can be determined under controlled temperature program in presence of nitrogen, air, vacuum or any other inert gas. Measurements that represent a loss in mass indicate sample's degradation while gain of mass shows reaction of a sample with air [113]. This method could be used to evaluate and compare stabilities, binding capabilities of different components blended to acquire hydrogels. In present work, development of binding forces among hydrogel components were assessed via TGA Q50 built in USA by Thermal Analysis Instrument. The 4.0 mg of dried sample was placed in platinum pan in inert atmosphere maintained by continuous purging of N_2 gas at flow rate of 10 mL/minute. The heating rate 10^oC/minute was maintained.

3.4.3 X-ray Diffraction (XRD)

XRD is an analytical technique frequently used for characterization of crystalline materials. It provides information about crystallinity, phases, particle sizes and grain sizes. It is also used to determine crystallinity in hydrogels to assess their strength and mechanical characteristics. Braggs equation is used for qualitative control over structure [114]. Constructive interference can be described by using Bragg's law, depicted in Equation 3.1.

$$2dSin\Theta = n\lambda \tag{3.1}$$

XRD analyses of fabricated hydrogels were performed by PANalytical diffractometer attached with Cu Kα radiations at wavelength of 1.544 Å. The 2θ range of working is 5-80^o.

3.4.4 Scanning Electron Microscopy (SEM)

SEM is a powerful technique that provides information about particle size, shape of powder and surface morphologies over a wide range of magnification. It requires very small volume of sample's spot focused by electron's beam. In SEM primary electrons are bombarded on the sample to eject secondary electrons from it. These secondary electrons are then attracted towards positive grid and detector receives signals in result which are amplified. It can be utilized to study surface topography, elemental analysis and porosity of hydrogels [115]. The surface morphology of SAR-15 and AgSD loaded SAR-15 (coded as DSAR-15) was determined by FE-SEM (JSM-6490A JEOL, Japan). Hydrogels were subjected to a process of gold-palladium sputter coating using a sputter coating instrument (JEOL JFC-1500, Japan) to impart the conductivity prior to analysis.

3.5 In-vitro Biodegradation

For biomedical applications, biodegradability of hydrogel is a fundamental precondition. Hence, biodegradability of hydrogels was investigated in proteinase-K solution. 0.2 mg/mL solution of proteinase-K was prepared in PBS [116]. Subsequently, 50 mg of each hydrogel was placed in 30 mL of above-mentioned enzyme solution. After 1, 3 and 7 days the gel was taken out from the solution. The surface water was removed with the aid of a filter paper and weight loss was computed by deduction of initial and final weights using Equation 3.2.

$$Biodegradation(\%) = \frac{w_1 - w_0}{w_0} \times 100 \tag{3.2}$$

Whereas, W_0 and W_1 are the weights of hydrogels before and after biodegradation, accordingly.

3.6 Swelling Analysis

Swelling is an important test not only to confirm hydrogel synthesis but also important for pH responsive release of therapeutic cargos. Thus swelling % of hydrogels were determined by placing 10 mg of each gel in distilled water, buffer solution and non-buffer solutions. After every 10 minutes the hydrogel was taken out from the aqueous solution and their surface water was removed by filter paper followed by weight measurement via sensitive balance [117]. The swollen hydrogel was again placed in the same solvent and the process was repeated till the establishment of swelling equilibrium. Following Equation 3.3 was used to compute the swelling %;

$$Swelling(\%) = \frac{w_s - w_d}{w_d} \times 100 \tag{3.3}$$

W_s and W_d symbolize the swollen and dry weights of hydrogel, correspondingly.

Non-buffer solutions of pH 2, 4, 6, 7, 8 and 10 were prepared by using 0.01M HCl and 0.01M NaOH. Likewise, buffer solutions of pH 2, 4, 6, 7, 8 and 10 were prepared from the buffer tablets marketed by BDH Laboratories London.

3.7 Cytocompatibility Assay

An examination of cytotoxicity of hydrogel samples were conducted using (3 - (4, 5-dimethylthiazol-2-yl) - 2,5-diphenyltet-razolium bromide (MTT) assay and human embryonic kidney (HEK-293) cell line. The cell cultures were cultivated in

dulbecco's modified eagle medium containing 10% fetal bovine serum [118]. The cultivation was done at 37 ^{o}C in CO_2 incubator.

Each individual well of a micro plate was occupied with a volume of 10,000 cells and 0.2 mL of dulbecco's modified eagle medium seeded on each hydrogel formulation followed by incubation for 24 hours.

Subsequently, each well poured with supplementary volume of 0.02 mL of MTT reagent to instigate the cellular reaction and engender formazan salts via the functioning of cellular mitochondrial dehydrogenases. After a reaction period of 2 hours at a temperature of 37 ^{o}C, the quantity of formazan salts was assessed at a wavelength of 450 nm employing a microplate reader [119].

The metabolic activities were then compared to those of HEK-293 cells that were employed as a growth reference in the absence of hydrogels. The cell viability was computed by using Equation 3.4;

$$Cell\ viability = \frac{Absorbance\ test}{Absorbance\ control} \times 100 \tag{3.4}$$

3.8 Antibacterial Assay

Agar-disc diffusion method against gram negative *E. coli* was brought into use for determining antibacterial activities of SAR-5, SAR-10, SAR-15 and SAR-20. Lysogeny broth (5 mL) was prepared at pH 7.4 followed by overnight incubation at 37 ^{o}C. On the other hand, hydrogel samples were placed in Whatman filter paper disc. In the next step, 15 mL of melted lysogeny agar was located on sterile petri plates for solidification and 50 μL of bacterial culture (*E. coli*) was poured and uniformly spread followed by incubation at 37 ^{o}C for 24 hours. Afterward, the zones of inhibition were calculated using micrometer [120].

3.9 In-vitro Encapsulation Efficiency (EE)

For EE, AgSD (100 mg) loaded hydrogel submerged in 50 mL of PBS solution at pH 7.4 at room temperature. After 24 hours, the solution was stirred for 10 minutes, filtered and the absorbance values were recorded by UV-visible spectrophotometer at 254 nm [121]. Percentage encapsulation was determined by equation 3.5 given below;

$$EE\,(\%) = \frac{Actual\ drug\ concentration}{Theoretical\ drug\ concentration} \times 100 \tag{3.5}$$

3.10 Drug Loading and Release

AgSD was loaded on SAR-15 hydrogel. For AgSD loading, CS/PEG homogenous blend was prepared as described in the section 3.3. Afterwards, 100 mg of AgSD was dissolved in 10 mL of methanol and added to the CS/PEG blend followed by agitation for additional 1 hour. After that, F-SEP (15 mg) was taken in 10 mL deionized water and sonicated up to 30 minutes followed by addition in blending mixture. The blend was agitated for 3 hours and followed the same procedure stated in section 3.3 to acquire DSAR-15 (AgSD loaded SAR-15).

For drug release experiment, 1M PBS solution was prepared and its pH was adjusted to 7.4 followed by autoclave sterilization. Subsequently, DSAR-15 was placed in 200 mL of PBS and after every 30 minutes the solution was drawn and subjected to the UV-visible spectrophotometer at wavelength of 254 nm. The quantity of AgSD release from the hydrogel was calculated from standard calibration curve.

3.11 AgSD Release Kinetics

The AgSD release kinetics with respect to time was studied by First order, Zero order, Higuchi and Korsmeyer-Peppas empirical models and their mathematical

forms are stated from Equation 3.6-3.9, respectively [122]. These models provide us mechanistic understanding and process involved in drug (AgSD) release from DSAR-15 hydrogel.

$$\text{First order model} \qquad logM_t = logM_o - \frac{kt}{2.303} \tag{3.6}$$

$$\text{Zero order model} \qquad M_t = M_o + K_o t \tag{3.7}$$

$$\text{Higuchi model} \qquad ft = QK_H \times t^{1/2} \tag{3.8}$$

$$\text{Korsmeyer-Peppas model} \qquad In\frac{M_t}{M_o} = nlnt + lnk \tag{3.9}$$

In above-mentioned mathematical equations, K, K_o and K_H are rate constants. On the other hand, M_o and M_t are the total loaded AgSD and AgSD released from hydrogel in time 't', correspondingly.

3.12 Statistical Analysis

The Origin Lab Corporation (Northampton, USA) produced Origin Pro 8.51 software, which was utilized for the statistical analysis of the numerical datasets and results. Statistical variances were calculated by Tukey test and one-way ANOVA. A $p < 0.05$ was considered significant and data is represented in mean ± standard deviation.

Chapter 4

Results

4.1 Scheme

The process of SEP modification, hydrogel fabrication and AgSD loading is briefly summarized in Figure 4.1 along with anticipated scheme.

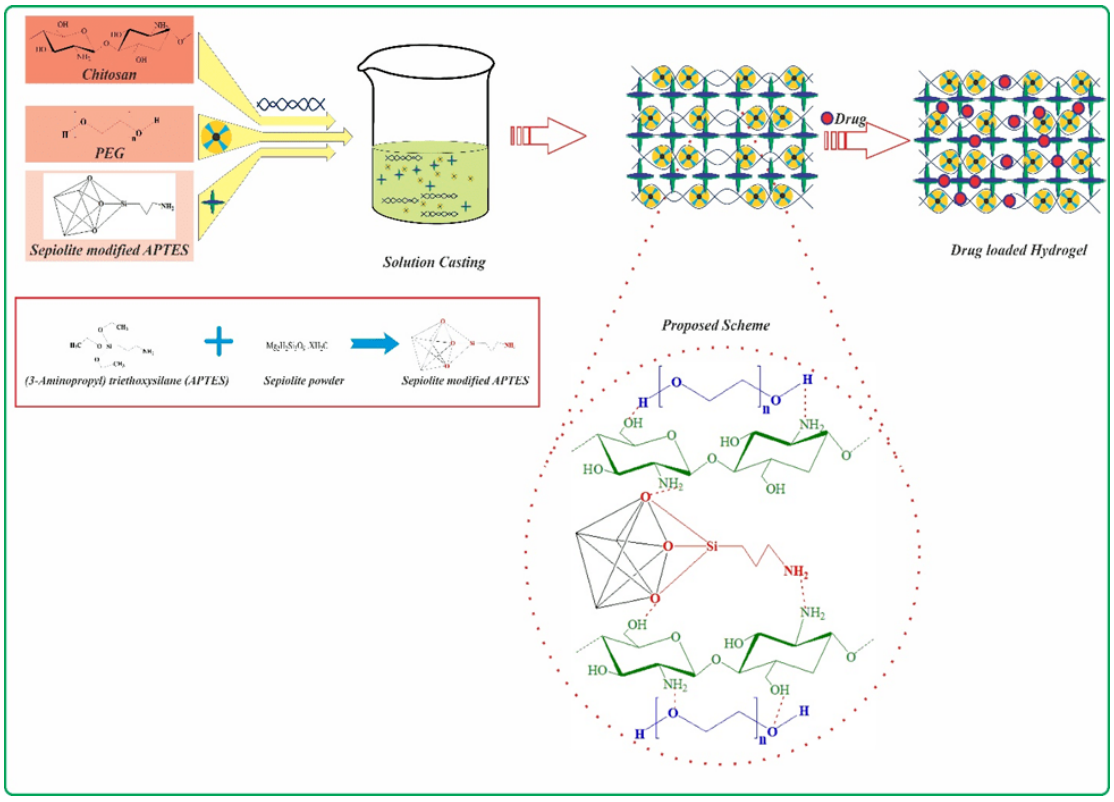

FIGURE 4.1: Graphical depiction of gel synthesis, SEP functionalization and proposed scheme.

4.2 Hydrogel Synthesis

In Figure 4.2, the pictures of F-SEP reinforced CS/PEG hydrogels are displayed using solution

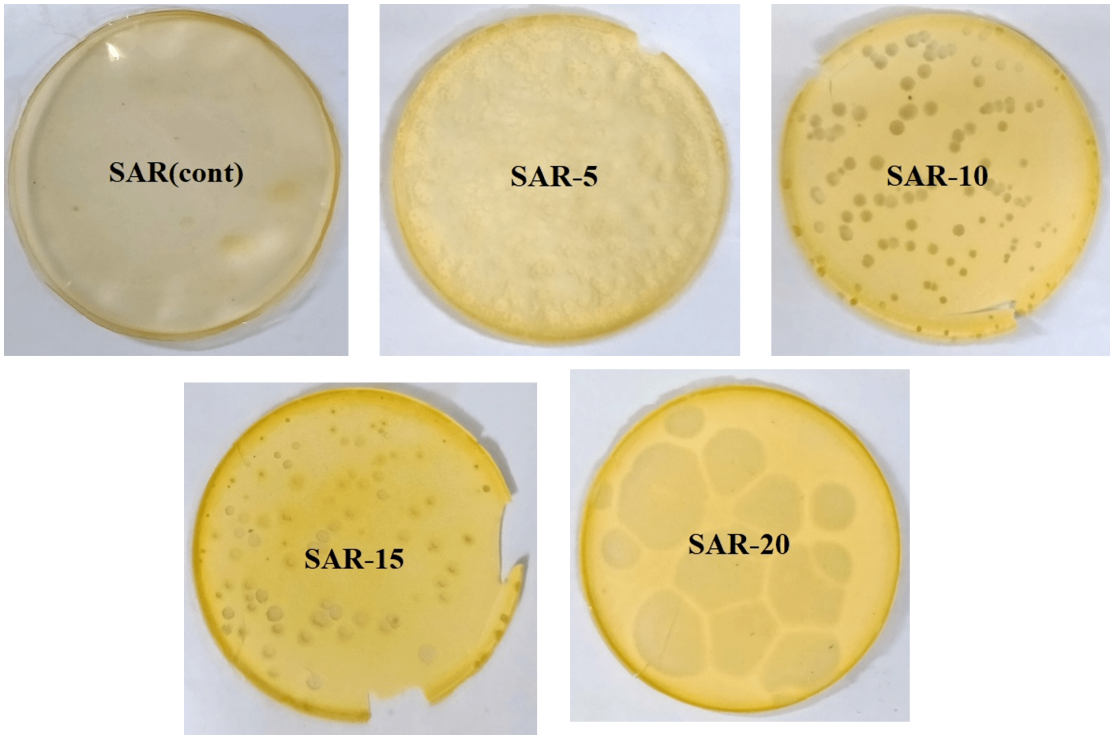

FIGURE 4.2: The images of prepared CS/PEG/F-SEP hydrogels.

4.3 FTIR

The successful SEP functionalization to acquire F-SEP is confirmed by the FTIR. The comparison of FT-IR spectrum recorded for F-SEP and non-functionalized SEP is displayed in Figure 4.3. On other hand, development of hydrogel interfaces by the interactions of functional groups among CS, PEG, and F-SEP are also established in FTIR analysis. Figure 4.4 reflects the FTIR spectrums for the fabricated hydrogels coded as SAR(cont), SAR-5, SAR-10, SAR-15 and SAR-20. In addition, establishment of siloxane linkages at 1021 cm^{-1} confirm the effective synthesis of hydrogels by mutable amount of F-SEP. However, this peak is absent in SAR(cont) due to the absence of F-SEP. The loading of AgSD on SAR-15 specimen is also verified by FTIR and represented in the Figure 4.5.

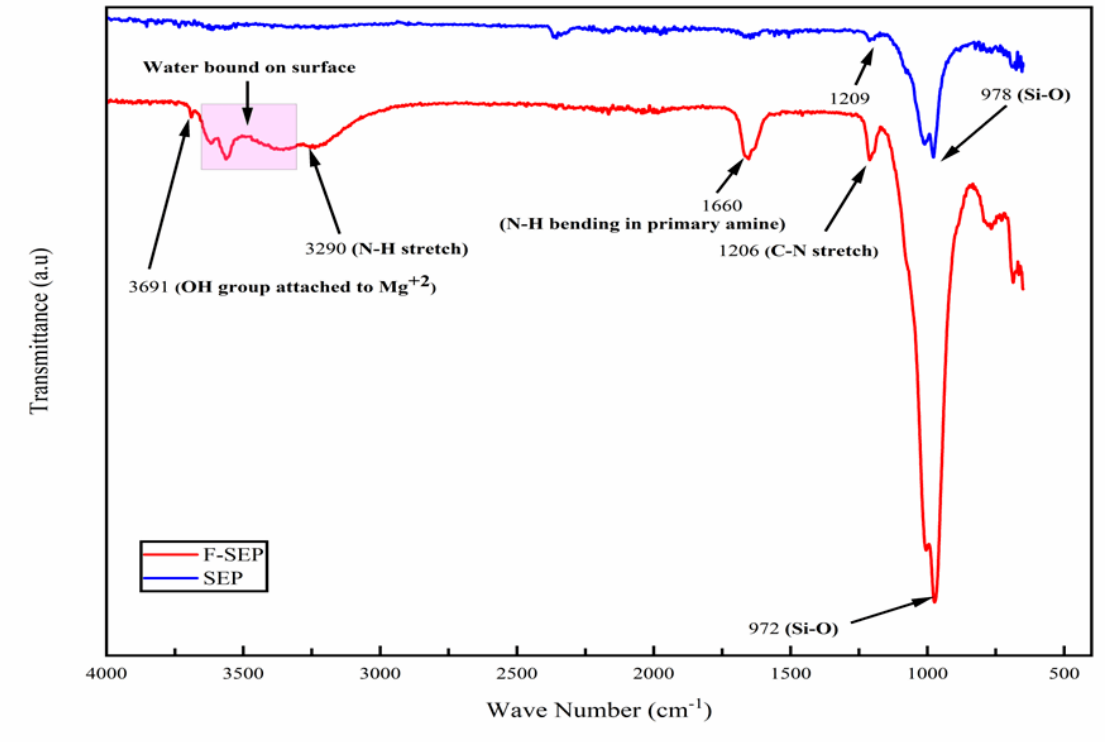

FIGURE 4.3: Functionalization of SEP with APTS to form F-SEP.

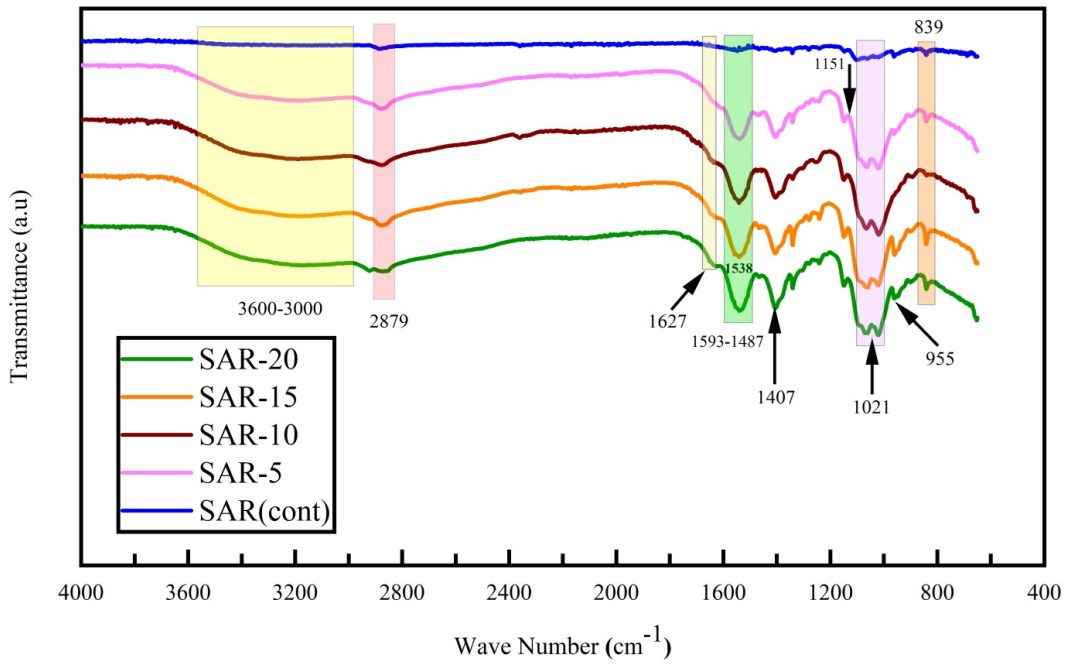

FIGURE 4.4: FTIR spectrums of synthesized hydrogels.

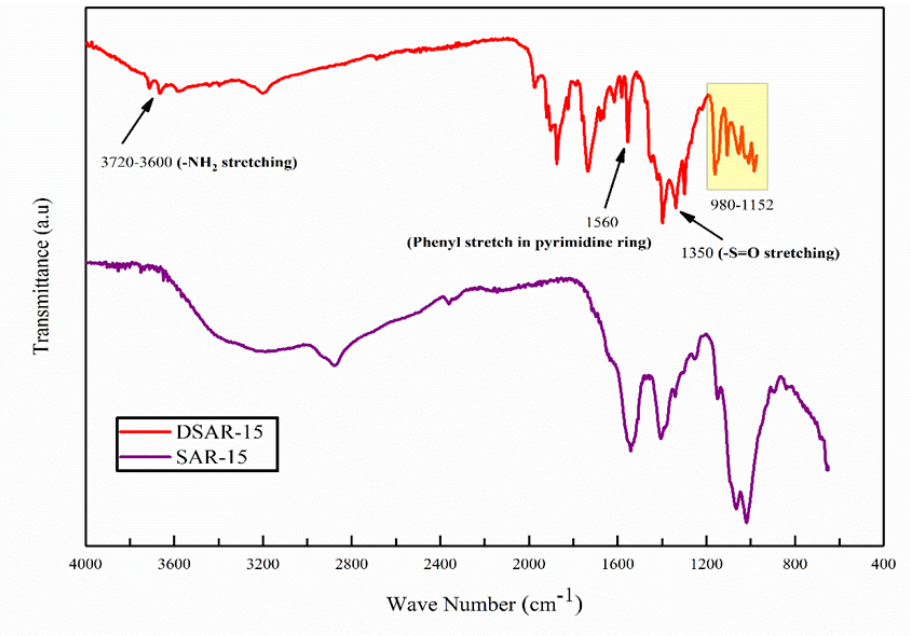

FIGURE 4.5: FTIR comparison of SAR-15 and DSAR-15.

4.4 Thermal Analysis

Thermal resilience of the fabricated hydrogels is analyzed by using TGA Q50. This test attests development of binding forces among hydrogel components by the variation in F-SEP quantity. In addition, it also confirms the claimed development of binding forces which are proportional to the quantity of F-SEP. In Figure 4.6, thermogram of SAR(cont), SAR-5, SAR-10, SAR-15 and SAR-20 are demonstrated which revealed that increase in SEP quantity directly influence the thermal stability. Weight losses (%) of synthesized hydrogels are appended in Table 4.1.

4.5 XRD Analysis

The pure CS, PEG and SEP reflect semi crystalline XRD patterns. CS shows two XRD peaks at 2 , 10^o and 20^o. However, XRD peaks of fabricated hydrogels are uniform and amorphous in nature where, the peak at 2 $=12^o$ is negligible. The XRD spectrographs are represented in Figure 4.7.

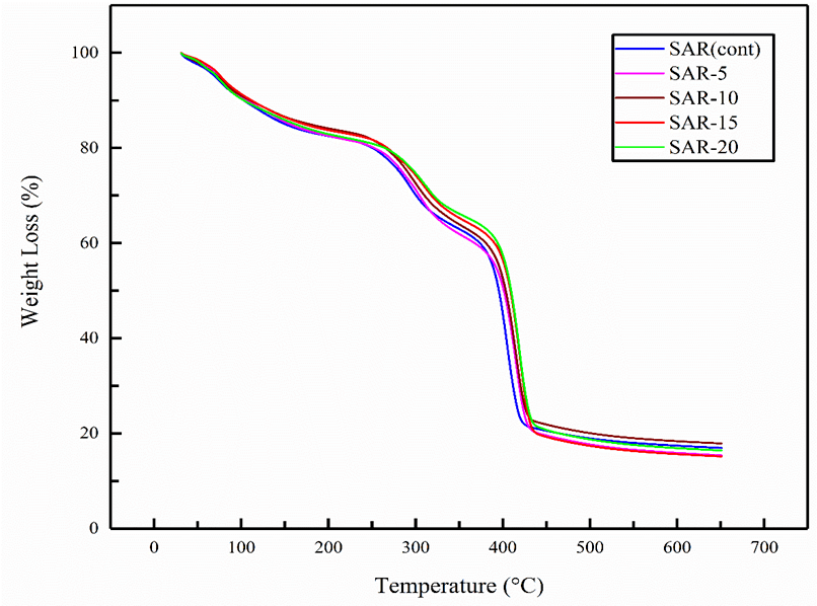

FIGURE 4.6: Thermal behavior of hydrogels in TG analysis.

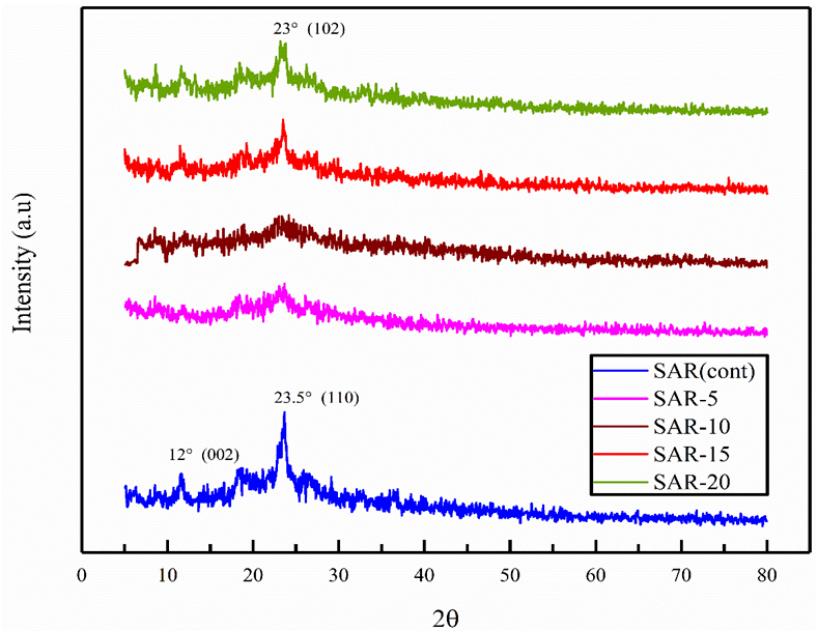

FIGURE 4.7: XRD peaks of fabricated hydrogels.

TABLE 4.1: Weight loss % of hydrogels in different temperature regions.

Temperature Zone (^{o}C)	**SAR(cont)**	**SAR-5**	**SAR-10**	**SAR-15**	**SAR-20**
30-100	9.62	9.23	8.98	8.64	9.62
101-400	50.06	43.95	42.20	38.18	36.38
401-650	37.57	30.24	34.02	26.84	28.58

4.6 Morphological Studies

The shiny and bright surfaces of SAR-15 and DSAR-15 are subjected to FE-SEM in order to acquire micrographs. As indicated in Figure 4.8, SEM micrographs of SAR-15 showcased highly porous, rough and heterogeneous surface.

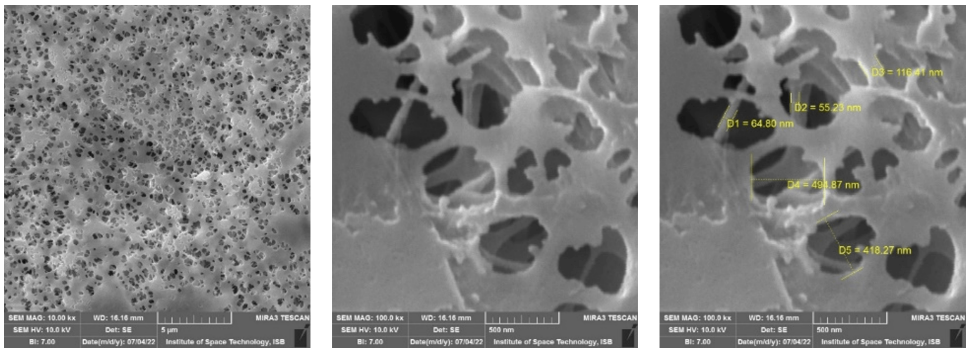

FIGURE 4.8: SEM micrographs of SAR-15.

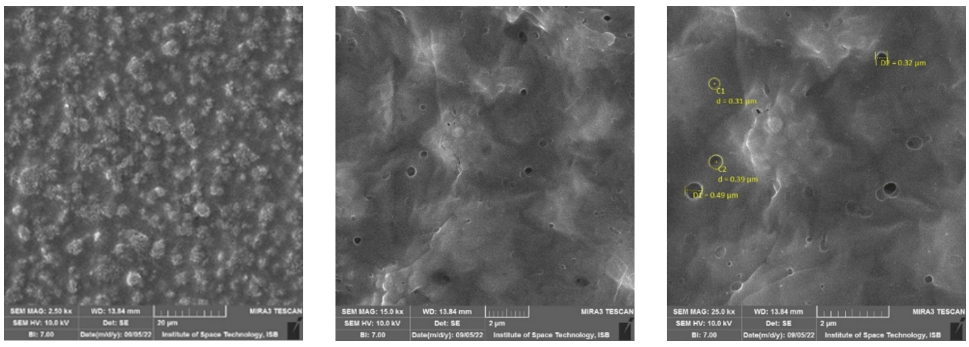

FIGURE 4.9: SEM micrographs of DSAR-15.

Loading AgSD in SAR-15 (coded as DSAR-15) displayed relatively even surfaces along with a considerable decrease in the pores displayed in Figure 4.9. Moreover, the drug molecules are also visible on the surface which endorsed AgSD loading in DSAR-15.

4.7 In-vitro Biodegradation

Biodegradation is prerequisite for any material to exploit it for medico-biological applications. Therefore, every hydrogel is immersed in proteinase-K enzyme solution prepared in PBS in order to observe their degradation capabilities. Resultantly, SAR(cont), SAR-5, SAR-10, SAR-15 and SAR-20 are biodegraded as 85, 86.2, 86.3, 87.5 and 92%, respectively in seven days. It is evident from Figure 4.10 that hydrogels are biodegradable and can be tainted by in-vivo enzymes. Moreover, degradation of hydrogels increased by the increase in the amount of F-SEP.

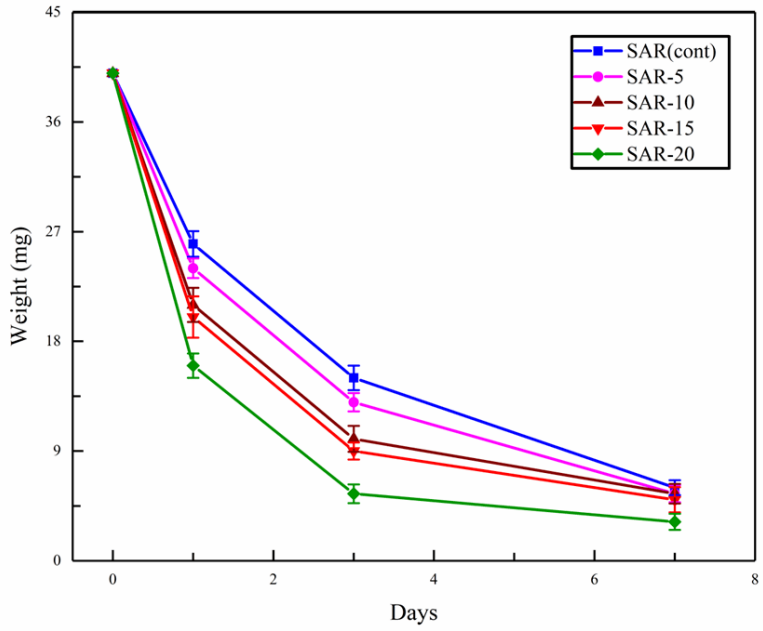

FIGURE 4.10: In-vitro biodegradation of hydrogels in enzymatic solution.

4.8 Swelling Analyses

Swelling ability is a unique characteristic of hydrogels in the presence of appropriate solvents. Hydrogels are capable to swell in aqueous solutions without dissolving in it which enables them to carry therapeutic cargos for their targeted and sustained release in drug delivery [123]. Thus, swelling profile of hydrogels are observed in distilled water, buffer/non-buffers and electrolytic solutions.

4.8.1 Swelling in Distilled Water

When hydrogels are subjected to pure distilled water, their swelling are increased as a function of time as shown in Figure 4.11. The swelling equilibrium is established at 140 minutes. Thereafter, no rapid increase in swelling volumes is observed. It is observed that swelling is proportional to the amount of F-SEP added in the gel. The reason why, SAR-20 reflected highest swelling (2544%) and SAP(cont) displayed lowest swelling (644%).

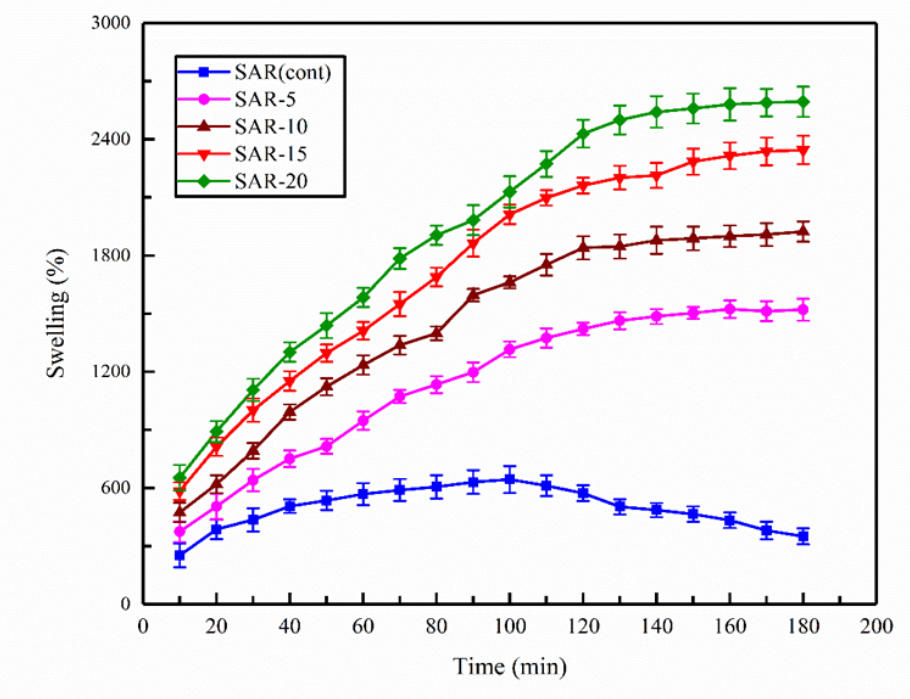

FIGURE 4.11: Swelling responses of hydrogels in distilled water.

The entry of water by inside hydrogels is governed by diffusion. The actual mechanism involved in the diffusion of water in hydrogels is determined by plotting calibration curves (shown in Figure 4.12) from swelling data using Equation 4.1. Where, F, k, t and n corresponds to the swelling, swelling rate constant, time taken by gel to swell and swelling exponent, respectively. The computed swelling factors are tabulated in Table 4.2. The value of "n" specifies the nature of diffusion process for captivation and release of water molecules. The prepared hydrogels followed quasi-Fickian diffusion model for entry/exit of water molecules because

the value of "n" is greater than 0.5 as provided in Table 4.2.

$$lnF = nlnt + lnk \tag{4.1}$$

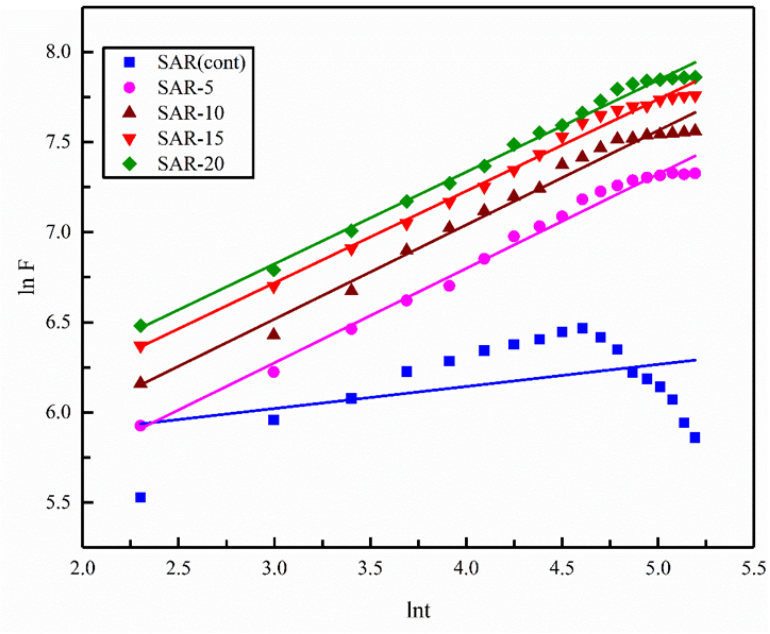

FIGURE 4.12: Calibration curves used to calculate diffusion factors.

4.8.2 Swelling in Non-buffers and Buffers

The swelling ability of hydrogels is influenced by different stimuli such as pH, temperature, osmotic pressure, electric and magnetic field. In drug delivery applications, usually pH targeting is preferred [124]. The reason why swelling % at different pH (2, 4, 6, 7, 8 and 10) are investigated in non-buffer and buffer solutions.

TABLE 4.2: Different diffusion factors calculated from swelling data.

Parameters	**SAR(cont)**	**SAR-5**	**SAR-10**	**SAR-15**	**SAR-20**
Adj. R-Square	0.107	0.986	0.982	0.995	0.991
R-Square (COD)	0.156	0.987	0.983	0.991	0.993
Pearson's r	0.399	0.993	0.991	0.995	0.996
Slope (n)	0.123	0.524	0.521	0.509	0.511
Intercept	5.655	4.712	4.951	5.191	5.295
k	285.716	111.274	141.316	179.648	199.338

In non-buffer solutions, hydrogels illustrated a pH responsive swelling behavior. In extreme acidic environment (pH 2) the swelling % are maximum. Apart from pH 2, increase in pH decreased the swelling volumes up to pH 6. At pH 7, the swelling volumes of hydrogels are better. In basic medium, swelling volumes are very limited as represented in Figure 4.13. All hydrogels reflected higher swelling at pH 2 and 7 which can be exploited for pH targeted release of drugs and development of drug loaded wound dressings [125]. In buffer solutions, the swelling profile of hydrogels is similar to that in non-buffer solutions as shown in Figure 4.14. However, in buffer solution swelling volumes are considerably lower as compared to the swelling % in non-buffer solutions at corresponding pH. For instance, the highest swelling % of SAR-20 in non-buffers and buffers at pH 2 is 4006 and 2950%, correspondingly.

4.8.3 Swelling in Ionic Media

Hydrogel's swelling is highly dependent upon nature, kind, charges and concentration of ions.

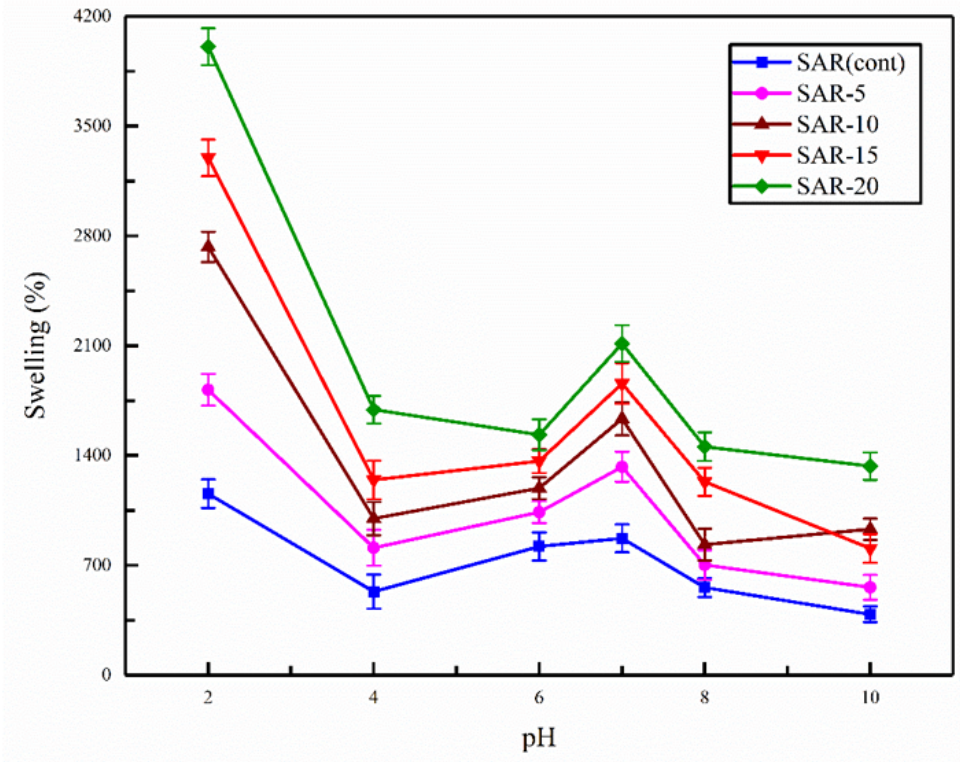

FIGURE 4.13: Swelling responses of hydrogels in non-buffers.

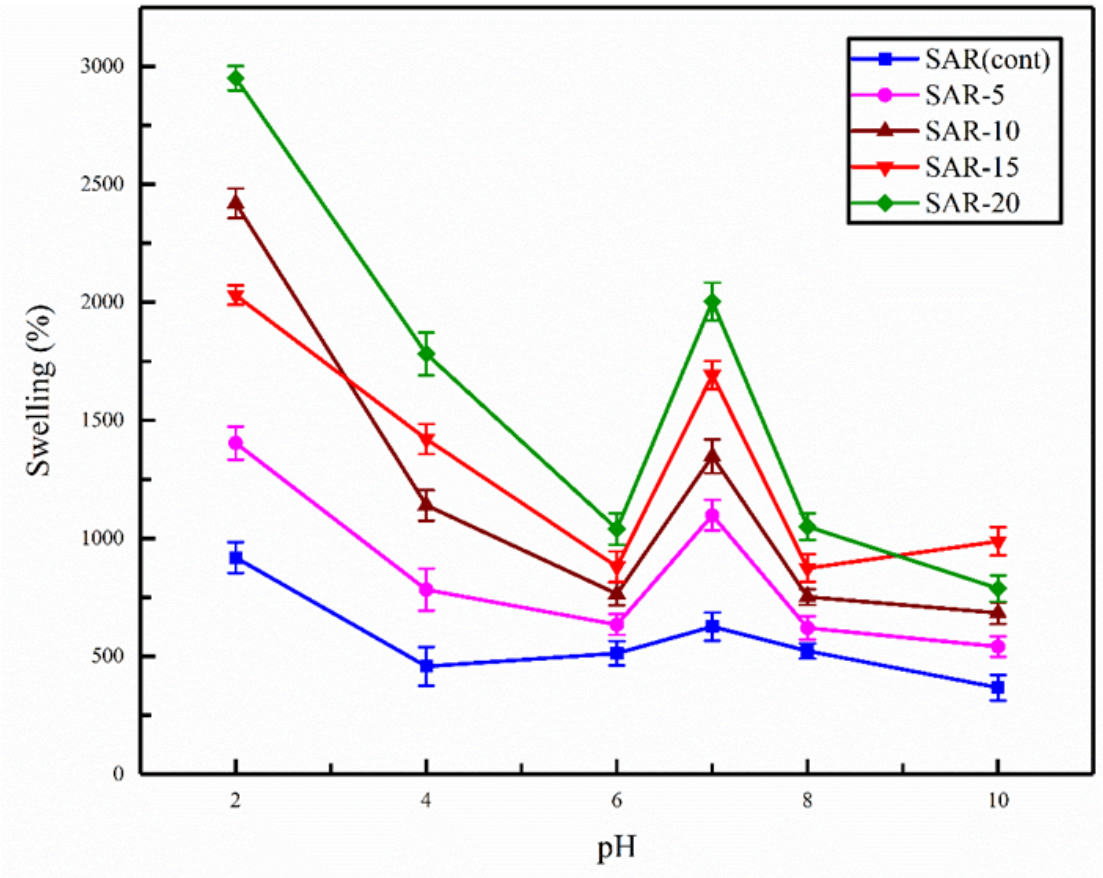

FIGURE 4.14: Swelling profiles of CS/PEG/F-SEP hydrogels in buffers.

In addition, these ions can also be encountered in in-vivo applications. Thus, swelling capacities of hydrogels are evaluated in variable strength of NaCl and $CaCl_2$ solutions. Both compounds have different cations and same anion which means their charge to size ratio is different (Ca^{2+} and Na^{1+}).

The recorded swelling responses of hydrogels are presented in Figure 4.15 and Figure 4.16. It is inferred from the comparison of Figure 4.15 and Figure 4.16 that swellings of CS/PEG/F-SEP hydrogels are inversely proportional to the molar concentration of NaCl and $CaCl_2$.

However, swelling responses in NaCl are relatively greater as compared to the $CaCl_2$ at any specific concentration. For example, swelling volumes of SAR-10 at 0.2M strength of NaCl and $CaCl_2$ are 1378 and 1120%, respectively.

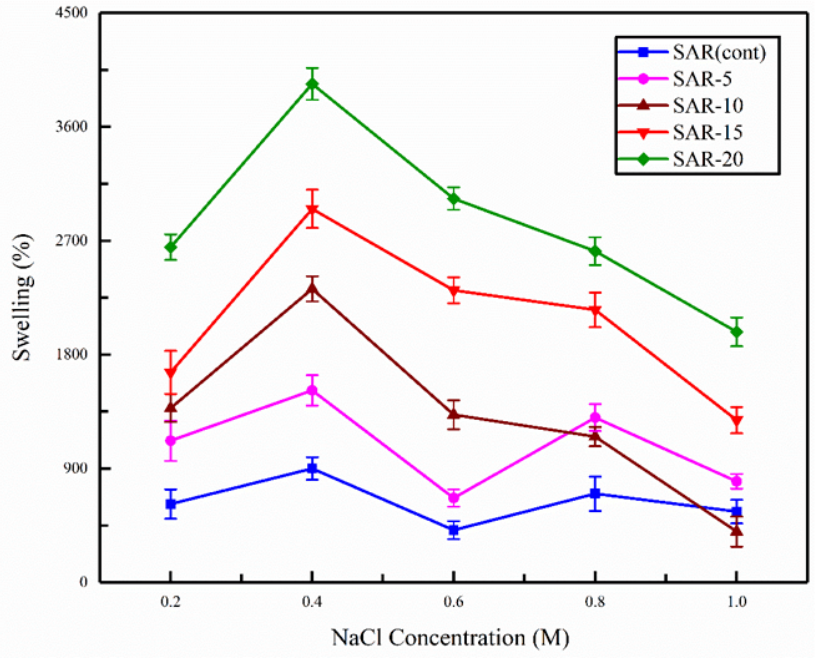

FIGURE 4.15: Swelling % F-SEP integrated CS/PEG hydrogels in NaCl.

4.9 Cell Viability Assay

Cell viability is very important for a hydrogels to further exploit them for in-vivo biomedical applications. Therefore, viability of F-SEP reinforced CS/PEG hydrogels are evaluated against HEK-293 cells using MTT assay.

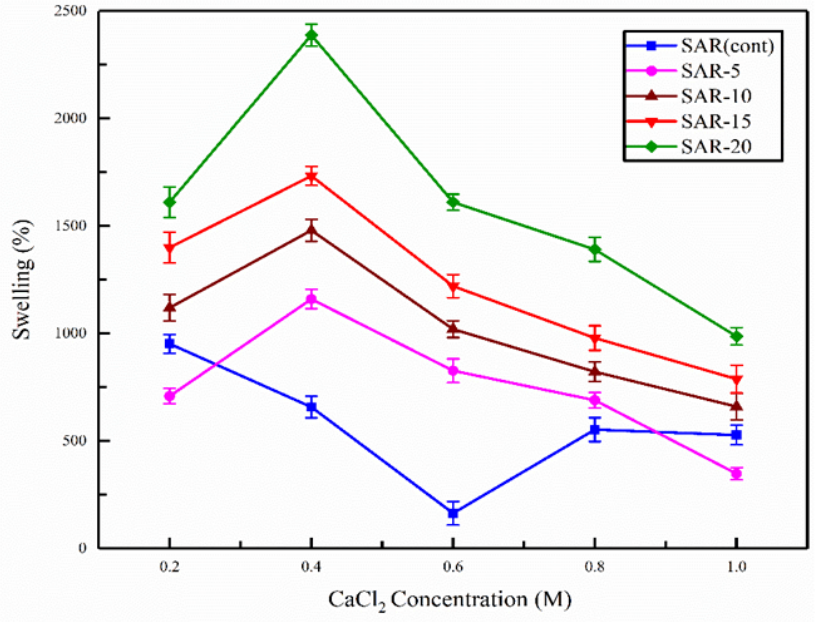

FIGURE 4.16: Swelling abilities of synthesized hydrogels in $CaCl_2$.

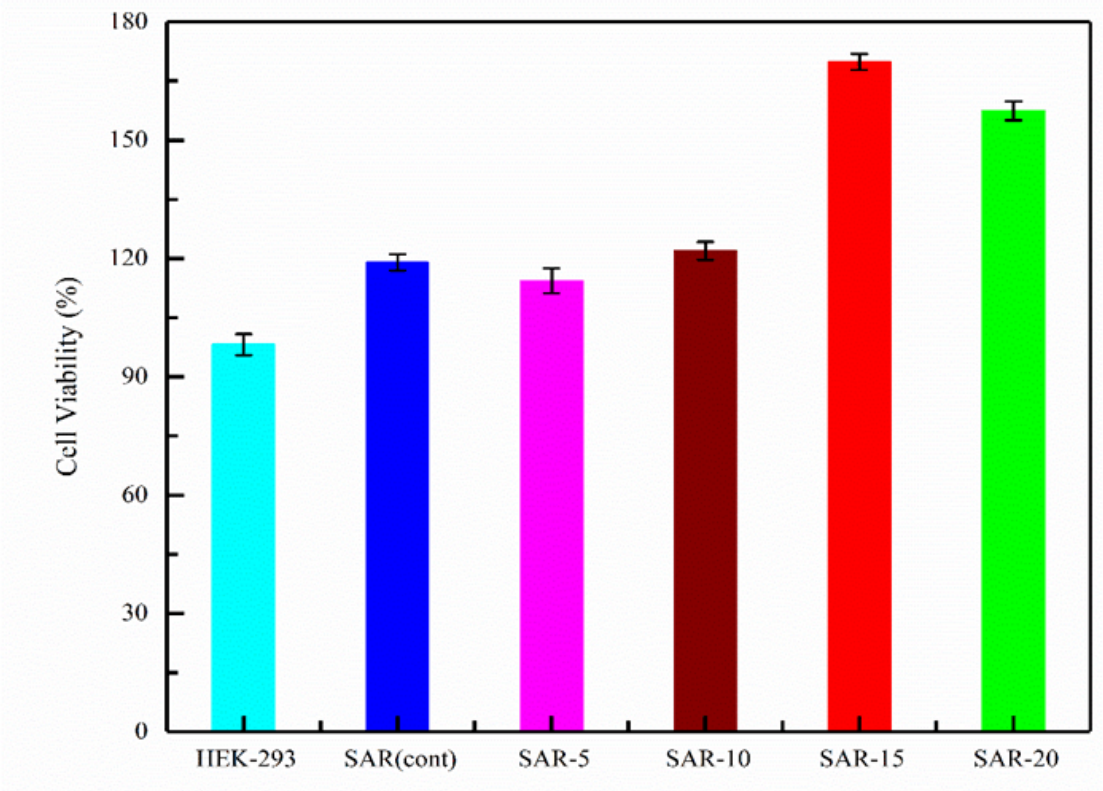

FIGURE 4.17: Viability of hydrogels against HEK-293 cell lines in MTT assay.

As a result 98.17, 119.0, 114.34, 121.94, 169.84 and 157.41% viabilities are observed for control (HEK-293 cells only), SAR(cont), SAR-5, SAR-10, SAR-15 and SAR-20, correspondingly. The results represented in Figure 4.17 confirmed cytocompatible, viable and non-toxic hydrogel platforms for drug delivery, wound dressing and other medico-biological applications.

4.10 EE%

100 mg of AgSD encapsulated SAR(cont), SAR-5, SAR-10, SAR-15 and SAR-20 are placed in 50 mL of PBS for 24 hours at pH 7.4. After that, the solution is stirred for 10 minutes and absorbance values are recorded by UV-visible spectrophotometer at 254 nm. The results of AgSD encapsulation are demonstrated in Figure 4.18. The maximum EE% is exhibited by SAR-15.

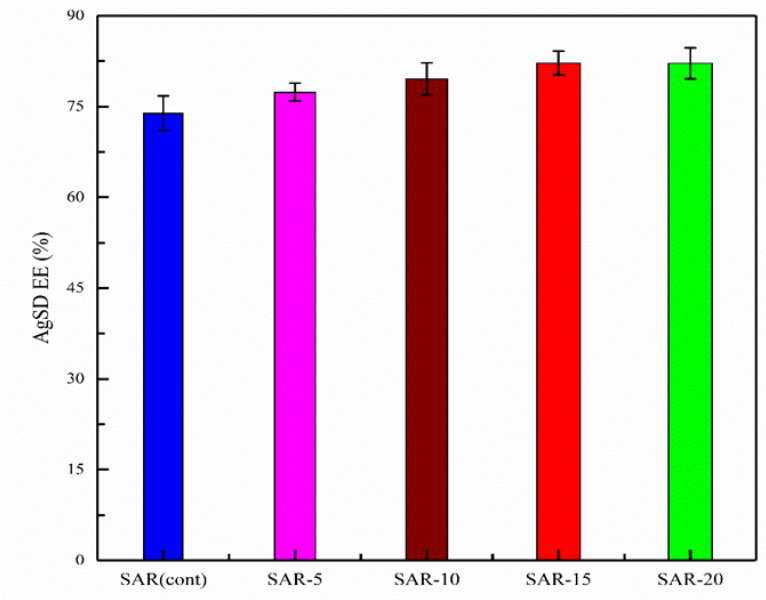

FIGURE 4.18: Hydrogels EE for AgSD.

4.11 Antibacterial Activity

Disc diffusion method is used to evaluate antibacterial activities of hydrogel samples against *E. coli*. The inhibition zones of SAR-5, SAR-10, SAR-15 and SAR-20 are 5.1 mm ± 0.1, 9.3 mm ± 0.2, 11.1 mm ± 0.1 and 15.2 mm ± 0.3, respectively (displayed in Figure 4.19).

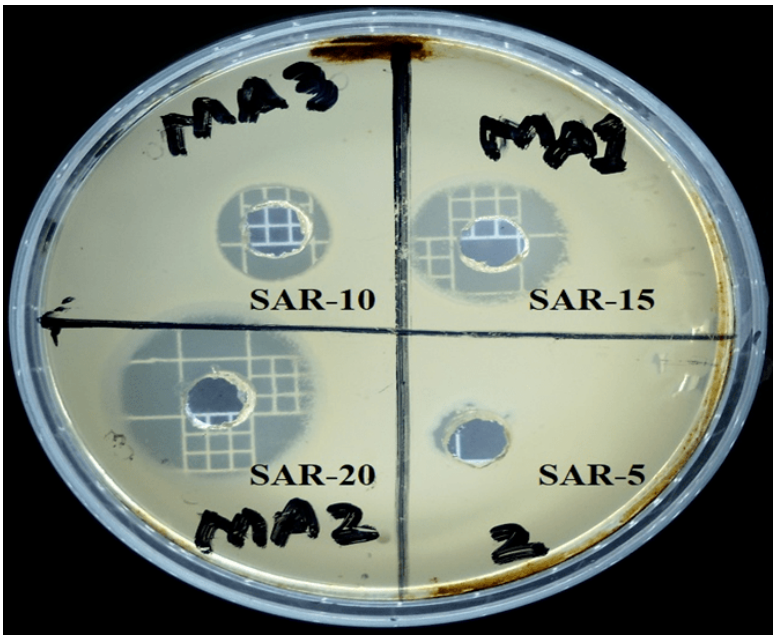

FIGURE 4.19: Antibacterial activity of hydrogels against *E. coli*.

4.12 AgSD Release

SAR-15 hydrogel is selected for release experiments because of its excellent swelling, higher EE%, good viability against HEK-293 cell lines and optimum degradation. DSAR-15 is taken in 200 mL of fresh and sterilized PBS (pH 7.4).

After every 30 minutes, 4 mL of the solution is drawn from beaker and recorded its absorbance value at 254 nm in UV-visible spectrophotometer (UV-1800, Shimadzu corporation Japan). By using standard calibration curve (shown in Figure 4.20), absorbance values are converted into concentration.

The release experiments are conducted three times and their average results are reflected in Figure 4.21 using error bars. In 30 hours, 81.27% of AgSD is released which confirmed its controlled release.

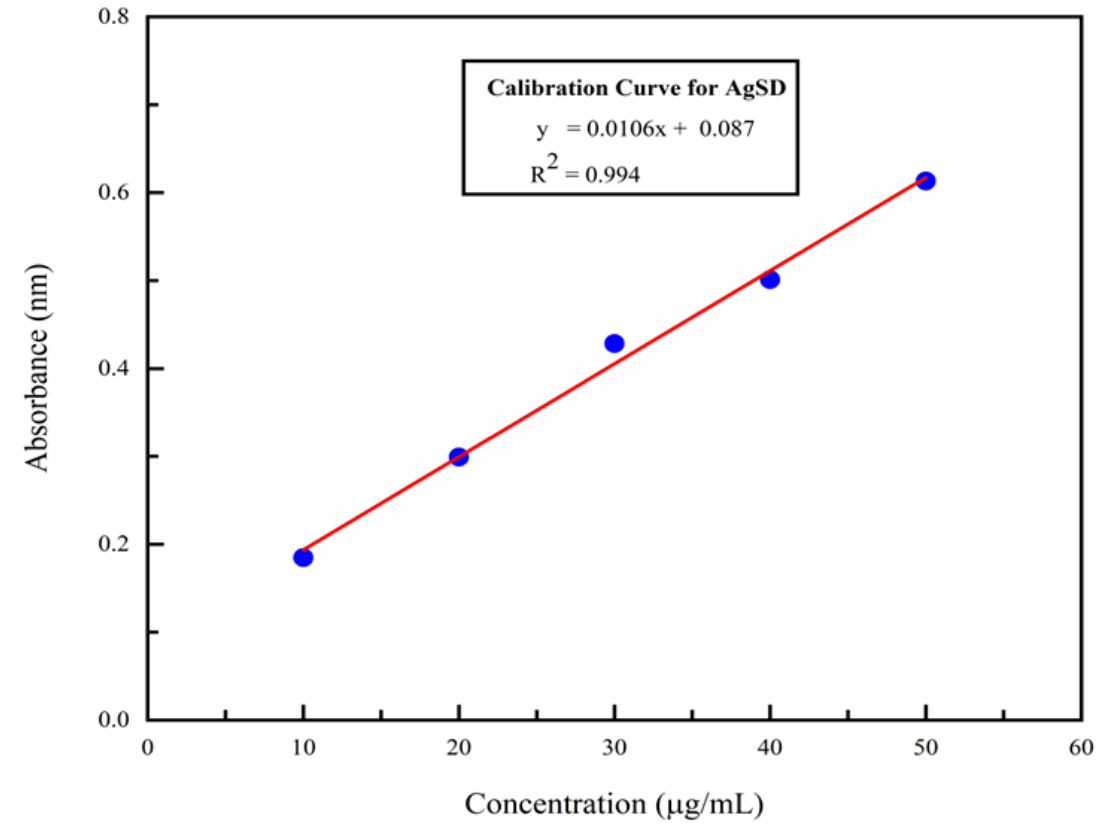

FIGURE 4.20: AgSD calibration curve used to convert absorbance date into concentration.

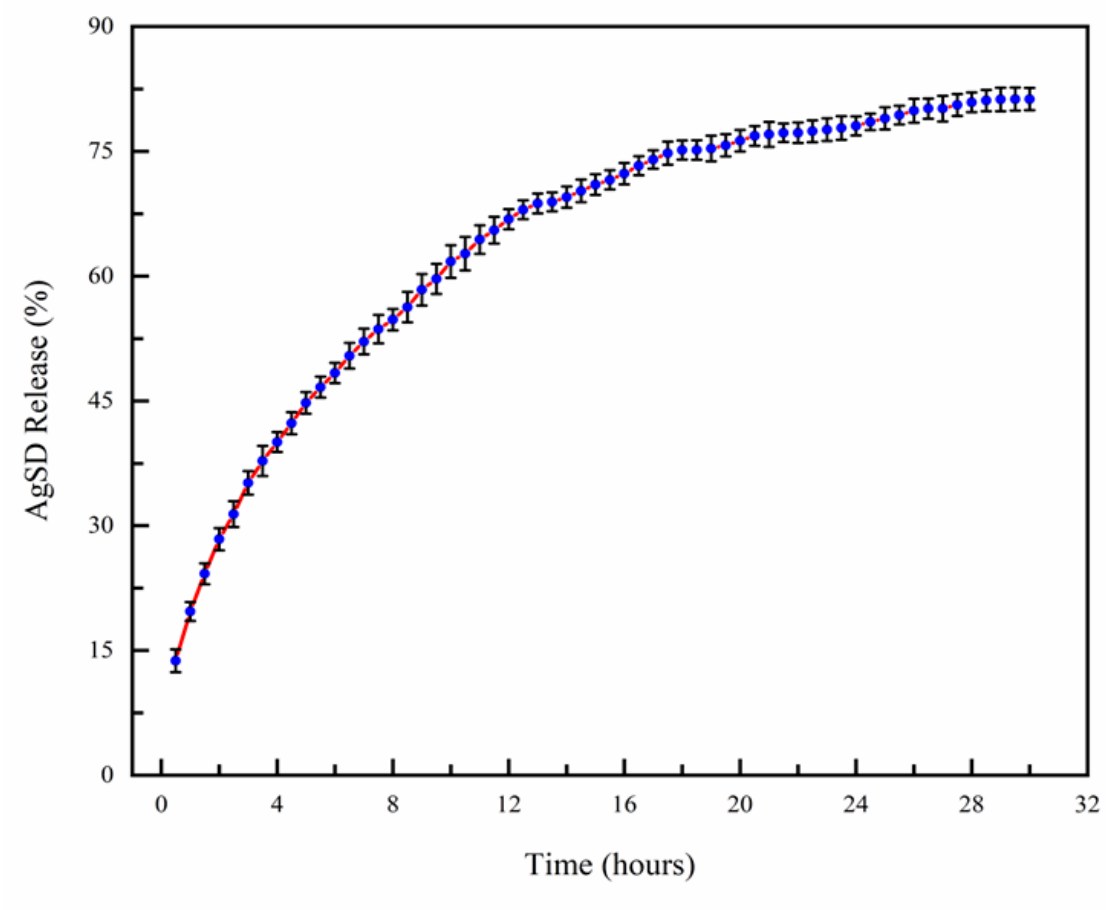

FIGURE 4.21: AgSD release % from DSAR-15 in PBS solution.

4.13 AgSD Release Kinetics

The data of AgSD release is applied to different kinetic models. The obtained fitting curves for First order, Zero order, Higuchi and Korsmeyer-Peppas models are depicted from Figure 4.22 - 4.25, correspondingly.

It is cleared from numerical values of regression coefficient (R^2) that Korsmeyer-Peppas model is obeyed by AgSD for release from DSAR-15 with highest value of R^2 (0.978). On the other hand, lowest R^2 value (0.694) is reflected for First order kinetic model.

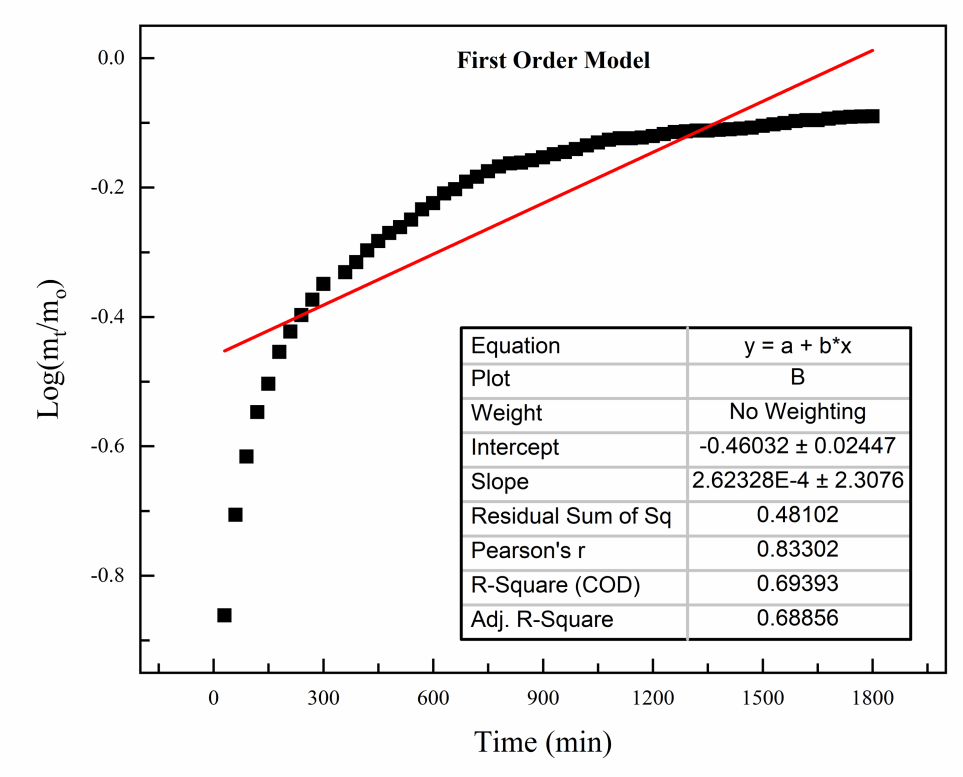

FIGURE 4.22: First order fitting curve for AgSD release.

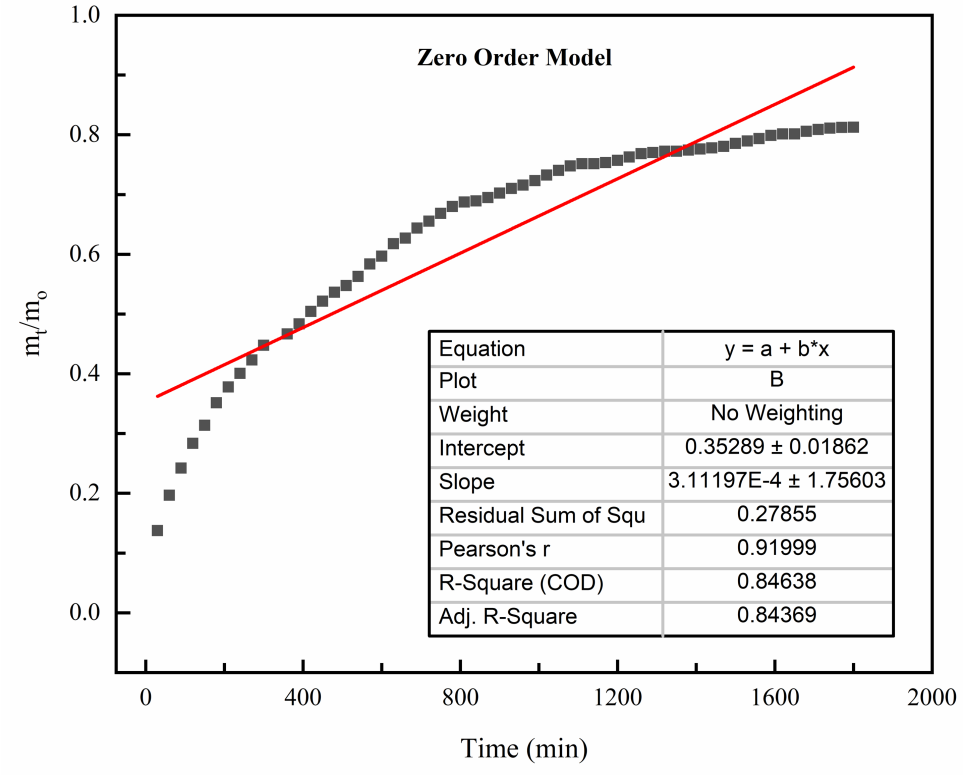

FIGURE 4.23: Zero order fitting curve for AgSD release.

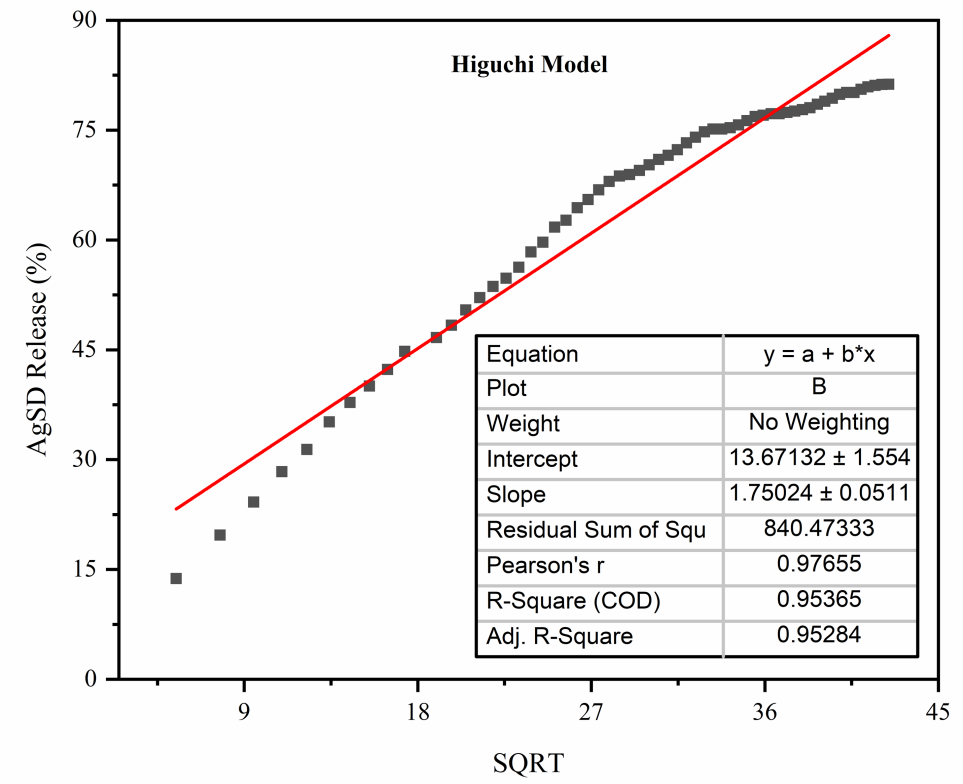

FIGURE 4.24: Higuchi model fitting curve for AgSD release.

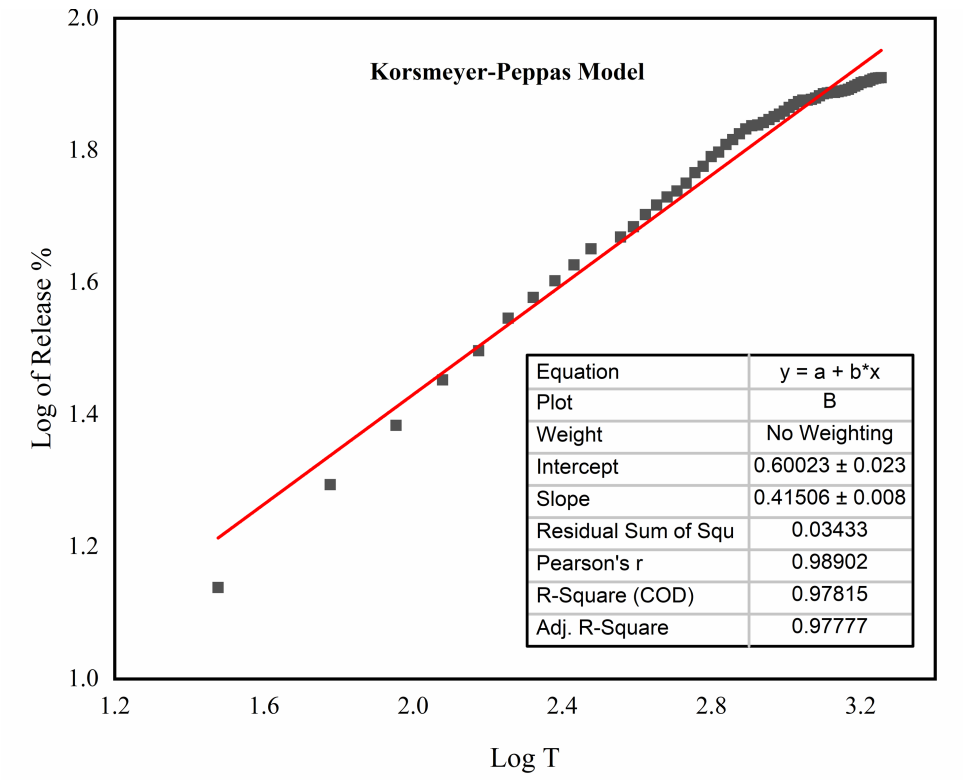

FIGURE 4.25: Korsmeyer-Peppas model fitting curve for AgSD releases.

Chapter 5

Discussion

5.1 Scheme

It is anticipated that amino-propyl groups present in APTS interacted with SEP to transform it into F-SEP. After that, this F-SEP is used for the fabrication of CS/PEG hydrogels. Amine groups (-NH_2) present in the CS and F-SEP played a key role in development of hydrogel matrices which is reflected with red dotted lines in the scheme represented in Fi gure 4.1.

5.2 FTIR

First of all, FTIR spectrum of SEP and F-SEP are compared in order to confirm SEP functionalization (displayed in Figure 4.3). Pure SEP clay is characterized by the bands ranged from 3000-3700 cm^{-1} due to the presence of Mg-OH (3690 cm^{-1}), zeolite water (3422 cm^{-1}) and coordinated H-O-H (3570 cm^{-1}). Further, the peak at 978 cm^{-1} are because of Si-O vibrations [126]. On other hand, the FTIR of F-SEP reflected more prominent peaks with relatively higher intensities. The peaks at 3691 cm^{-1}, 3565 cm^{-1} and 3290 cm^{-1} correspond to the Mg-OH, bound water and N-H stretching, correspondingly. In addition, N-H stretching peak at 3290 cm^{-1} and N-H bending vibrations due to the presence of primary amine at 1660

cm^{-1} are absent in pure SEP. Moreover, the bands due to C-N stretch (1206 cm^{-1}) and Si-O (972 cm^{-1}) stretch reflected decrease in wave number that confirms the increase in the mass of vibrating groups as compared with non-functionalized SEP. The emergence of new peaks, higher intensities of the FTIR spectrums and shift in peaks from 1209 cm^{-1} and 978 cm^{-1} confirms the synthesis of F-SEP using APTS.

The IR spectrum of SAR(cont), SAR-5, SAR-10, SAR-15 and SAR-20 is shown in Figure 4.4. The broad band in the region from 3000-3700 $cm^{-1}$is because of –OH stretching originated from the CS (-OH), SEP (Mg-OH) and PEG (-OH) [127]. Polymer linked –CH stretching is also evident at 2879 cm^{-1} which confirms the presence of PEG and CS in the fabricated hydrogels [128]. The presence of pyronose ring, saccharine and amide groups are the characteristic IR peaks of CS. The IR region from 1487-1593 is because of amide groups present in the CS-based hydrogels [129]. The presence of pyranose and saccharine are confirmed by peaks at 839 cm^{-1} and 1151 cm^{-1}, correspondingly. The peak at 1021 cm^{-1} is present in each hydrogel sample except SAR(cont). This peak is due to the development of siloxane linkage (Si$\cdots$O$\cdots$Si) developed due to the presence of F-SEP. The Si-groups present in F-SEP (inherited from APTS) are accountable for development of this linkage. However, this peak is absent in SAR(cont) because control sample lacks F-SEP in it. Furthermore, the Si-O peak at 974 cm^{-1} present in pure SEP is shifted to the lower intensity 955 cm^{-1}. The peak at 1627 is attributed to the N-H bending vibration due to primary amine group. On the basis of afore-mentioned discussion, it is inferred that all components of the CS/PEG/F-SEP hydrogels are present and also interacted productively to produce hydrogels.

In the same liking manner, the IR spectrum of DSAR-15 (AgSD loaded SAR-15) and SAR-15 are compared in Figure 4.5 to confirm presence of AgSD drug in hydrogel specimen prior to the release studies. The DSAR-15 demonstrated similar peaks as shown by SAR-15. However, the presence of amine (-NH2 stretch) group, pyrimidine ring and sulfonamide stretch (S=O) are established by the additional peaks at 3720-3600 cm^{-1}, 1560 cm^{-1} (phenyl stretch) and 1350 cm^{-1}, respectively. Similarly, some other peaks related to the AgSD are also emerged and highlighted

in the IR spectrum of DSAR-15 that confirmed AgSD loading in SAR-15 to acquire DSAR-15.

5.3 Thermal Behavior

TG curves of hydrogels are demonstrated in Figure 4.6. It is observed that increase in F-SEP quantity directly influenced the thermal resilience. This may be explained by the development of Vander Walls forces, hydrogen bonding and siloxane interactions among CS, PEG and F-SEP. SAR(cont), SAR-5, SAR-10, SAR-15 and SAR-20 revealed three phase decomposition which is characteristic of CS [130]. First decomposition phase range from 20-100 ^{o}C which mainly involves evaporation of gel bound water. The second phase 101-400 ^{o}C corresponds to the primary CS decomposition along with loss of acetyl functionalities. It is the major degradation zone [131]. Generally, the pure CS displays two decomposition zones up to 450 ^{o}C. However, development of hydrogel interfaces may have enhanced stability of CS skeleton. In consequence, third decomposition zone of polymeric residue containing CS/PEG/F-SEP is recorded at 401-650 ^{o}C. It is important to note that pure CS represent second degradation phase in the regions of 102-275 ^{o}C [132]. However, incorporation of F-SEP and PEG significantly enhanced the thermal stability as the second stage degradation shifted from 102-275 ^{o}C to 102-400 ^{o}C [133]. The weight loss % of F-SEP cross-linked CS/PEG hydrogels are provided in Table 4.1.

5.4 XRD Analyses

XRD pattern of pure CS and PEG are semi-crystalline. CS represents two major peaks at 2θ, 10^{o} and 20^{o} [134]. Likewise, two XRD peaks at 19^{o} and 23^{o} appear for PEG. In contrast, SEP demonstrates crystalline XRD peaks with higher structural order showing diffraction peaks at 7.9^{o}, 28.4^{o} and 34.9^{o} [135]. However, diffraction peaks recorded for hydrogels (displayed in Figure 4.7) are uniform and amorphous. This endorsed efficient blending and compatibility of ingredients used to synthesize

hydrogel (CS, PEG and F-SEP). In SAR(cont) which lacks F-SEP, two peaks are evident at 12^o and 23.5^o. Conversely, in F-SEP containing specimens, the diffraction maxima at 12^o is negligible while, the peak at 23.5^o is shifted to 23^o corresponds to the (102) plane. This might be explained by the increase in binding in CS/PEG in hydrogel due to the addition of F-SEP [136].

5.5 SEM Analyses

The shiny surface of SAR-15 and DSAR-15 are analyzed by using FE-SEM. Figure 4.8 corresponds to the SAR-15 hydrogel which indicated diverse and highly porous surface. The average diameter of the pore is 64-116 nm. These pores are very critical in the entry exit of water and also for sorption/desorption of drugs. In comparison to the SAR-15, the DSAR-15 surface appeared to be heterogeneous, rough and bumpy as depicted in Figure 4.9. It also contains multi-faceted spots and pores. But, the pores are few in number and relatively greater in diameter. The average diameters of the pores are 320-500 nm.

The AgSD probably adsorbed on the entire surface by occupying pores in the gel matrix. Accordingly, numbers of pores in the DSAR-15 are rare with greater diameter. The difference in the morphological appearance and porosity is mainly because of the presence of AgSD which is uniformly adsorbed on the entire surface. The larger and less numbers of pores are critical in the entry of solvent molecule in DSAR-15. Resultantly, the intermolecular forces among hydrogel and drug are tainted to offer controlled and sustained release.

5.6 In-vitro Biodegradation

Degradation test is a prerequisite for employment of materials in medico-biological systems. F-SEP incorporated CS/PEG hydrogels reflected excellent degradation in proteinase-K solution made in prepared in PBS (displayed in Figure 4.10). As a result, maximum degradation is shown by SAR-20 (92%) in seven days.

The results indicated that incorporation of F-SEP in CS/PEG gel enhanced the degradation %. F-SEP introduction into CS/PEG matrix significantly improved hydrophilic and water absorbing capability due to the increase in number of amine (-NH2) and hydroxyl (-OH) groups. For that reason, dissolution or solublization is the operating phenomenon for biodegradation behavior of hydrogels. In other words, greater water loving environment promotes absorption of water inside hydrogel which eventually stimulated degradation. This effect is further pronounced in the presence of enzyme. CS is naturally biodegradable polymer which offers acetyl moieties to bind with proteinase-K enzyme. Consequently, it is broken into smaller polysaccharides which are useful in metabolic reactions.

5.7 Swelling Analyses

In this section swelling responses of F-SEP reinforced CS/PEG hydrogels are discussed in detail.

5.7.1 Swelling in Distilled Water

The swelling responses in Figure 4.11 are increased by the increase in F-SEP quantity which endorsed the enhancement of hydrophilic nature among hydrogel elements (CS, PEG, F-SEP) [137]. The maximum swelling (2594%) is exhibited by SAR-20 comprised 20 mg of F-SEP while minimum swelling (351%) volumes are observed for SAR(cont) which lacks F-SEP. It is evident that swelling responses are function of F-SEP. This might be due to the increase in the hydrophilic behavior of hydrogels inherited from amine, hydroxyl and zeolitic water found in F-SEP also corroborated from FTIR. The diffusion is the process responsible for entry and exit of solvent molecules from hydrogels. The diffusion factors computed by using calibration curves for each specimen (depicted in Figure 4.12) are provided in Table 4.2 which confirmed that the value of "n" in accordance with $0.5 < n < 1$ for SAR-5, SAR-10, SAR-15 and SAR-20. Therefore, non-Fickian diffusion mechanism is obeyed [138]. In contrast, SAR(cont) that lacks F-SEP, has the

n > 0.5. Hence, quasi-Fickian diffusion process is conformed. In conclusion, SAR(cont) followed quasi-Fickian diffusion but addition of F-SEP in CS/PEG altered the diffusion mechanism into non-Fickian process. In order to compare kind of diffusion mechanism involved on the basis of swelling exponent (n), Table 5.1 is provided below;

TABLE 5.1: Swelling exponents "n" and diffusion mechanism.

Type of Diffusion	**Swelling Exponent (n)**
Quasi-Fickian diffusion	n <0.5
Fickian diffusion	0.5
Anomalous (non-Fickian) diffusion	0.5 <n <1.0
Non-Fickian case-II zero order	1
Non-Fickian super case-II	n >1.0

5.7.2 Swelling in Non-buffer and Buffers

In non-buffer and buffer solution the swelling responses of hydrogels are very high at pH 2 as demonstrated in Figure 4.13 and 4.14, correspondingly. This is attributed to the protonation of amine and hydroxyl groups (present in CS, PEG and F-SEP) at pH 2 and similar charges repel each other and create room for inward movement of water. Resultantly, higher swelling volumes are recorded at lower pH [139]. Further, increase in pH deceased protonation of amine and hydroxyl functional groups and swelling volumes are reduced. Again at pH 7, swellings of hydrogels are higher due to the presence of uncharged groups which perhaps relaxed polymeric chains and inward flow of water improved their swelling. In basic medium, recorded swelling capacities of hydrogels are even very low. This is attributed to the de-protonation of the group that inculcated stronger interactions among hydrogel components which minimized inside diffusion of water [140].

It is important to note that, higher swelling responses are detected in non-buffer solution as compared to buffer solution because buffer solution hold greater ionic concentration and charge imbalance. For instance, SAR-20 exhibited highest swelling 4006% and 2950% at pH 2 in non-buffer and buffer solutions, respectively.

Hydrogels reflected different swelling volumes as function of pH. Therefore, it is confirmed from the Figure 4.13 and Figure 4.14 that prepared F-SEP cross-linked CS/PEG hydrogels are pH responsive. F-SEP clay influenced the swelling, thermal and degradation capabilities [141].

5.7.3 Swelling in Ionic Solutions

It is observed that CS/PEG/F-SEP hydrogels displayed inverse relation of swelling volumes to the molar concentration of ions (Na^{+1} and Ca^{+2}). This is because increase in active masses of ions strongly interacted with polymeric chains and promoted inter-molecular forces. Hence, water captivation is reduced as function of NaCl strength as shown in Figure 4.15. This is in strong agreement to the studies reported in literature [142].

In Figure 4.16, this effect is more pronounced in the $CaCl_2$ solution which resulted in more decrease in swelling % as compared to NaCl. Moreover, Ca^{+2} ions are bivalent and generate polymeric chelating. Thus, inferior swelling volumes are recorded [143]. The swelling % recorded for SAR-20 and SAR-15 in NaCl at 0.2M concentration are 2650% and 1660%, respectively. While in $CaCl_2$ at 0.2M concentration, 1600% and 1411% are observed for SAR-20 and SAR-15, correspondingly.

5.8 Cell Viability Assay

Cell viability assay (In Figure 4.17) reflected higher values of viability % for each hydrogel relative to the control group (HEK-293 cell lines) after 24 hours in MTT assay. The increase in F-SEP quantity provided more productive environment for the cells to replicate, the reason why viability (%) are increased. The maximum viability % is noticed for SAR-15 (169.84% $\pm$ 2.02) sample which is comprised of 15 mg of F-SEP clay. However, further increase in F-SEP decreased viability % in SAR-20 up to (157.41% $\pm$ 2.39). Based upon the results, it is inferred that formulated CS/PEG/F-SEP hydrogels do not produce any cytotoxic response

in HEK-293 cells which also encourage their utilization in drug delivery, wound dressing, tissue engineering and sustained release applications.

5.9 EE%

The outcomes of EE % are reflected in Figure 4.18. SAR(cont) specimen has lowest EE of 73.87% ± 2.86. In contrast, SAR-5, SAR-10, SAR-15 and SAR-20 shown higher EE% 77.34% ± 1.48, 79.56 ± 2.66, 82.17 ± 1.99 and 82.13 ± 2.57 for AgSD encapsulation, accordingly. SAR-15 and SAR-20 exhibited highest EE% among all samples. The results indicated that by the increase in the amount of F-SEP clay, the amount of encapsulated drug is increased probably due to the interaction among polar functionalities present in AgSD, CS, PEG and F-SEP.

5.10 Antibacterial Action

The results of bactericidal actions of hydrogels against *E. coli* are stated in Figure 4.19. SAR-20 exhibited maximum antibacterial activity against *E. coli* with inhibition zones 15 mm ± 0.3. The antibacterial activity of F-SEP incorporated CS/PEG hydrogels is credited to the amine group present in CS. This group is also present in F-SEP (APTS functionalized SEP) which is the probable reason behind increase in the antibacterial action from SAR-5 to SAR-20 against *E. coli*. Antibacterial action of CS-based hydrogels is explained in two ways in the literature. Firstly, CS and bacterial DNA binding occurs that might prevent transcription and translation [144]. Secondly, a gram negative bacterium consists of phospholipids and lipopolysaccharides; as a consequence, these impart negative charge on the surface of bacteria [145]. Therefore, interactions among gram negative bacterial membrane and NH3+ moieties found in CS takes place that may result in significant alterations in cell membrane and restrict bacterial growth [146].

5.11 AgSD Release

The calibration curve used to compute amount of drug release is stated in Figure 4.20. The release profile of AgSD from DSAR-15 is reflected in Figure 4.21. In the beginning, faster AgSD release is observed because of swelling. Almost 28.35% and 50% of AgSD is released in 2 hours and 6.5 hours, correspondingly. The initial and relatively faster release of AgSD is credited to the swelling process. Later on drug release is slower and controlled by the diffusion process. Altogether, 81.27% AgSD is released in 30 hours which in strong agreement to US pharmacopeia standards. The DSAR-15 exhibited better sustained release profile of drug as compared to previously reported studies. The cumulative release % reflected more sustained release at physiological pH relative to the already reported studies in literature represented in Table 5.2. Henceforth, F-SEP cross-linked CS/PEG hydrogels could be an efficient platform for drug loaded wound dressings for wound healing applications.

TABLE 5.2: Comparison of AgSD cumulative release profile from CS-based hydrogel films.

Hydrogel	**Technique**	**Release (%)**	**Time (h)**	**Application**	**Ref**
CS/Alg scaffold	3D printing	100	5	Wound healing	[147]
CS/PVA	Freeze-thawing	75	12	Burn dressing	[148]
CS/PVA/Dextran	Cryogelefication	90 <	2	Transdermal delivery	[149]
CS/pectin	Polyelectrolyte	99	24	Wound dressing	[150]
CS/gelatin	Solvent casting	77	12	Wound treatment	[151]
CS/PEG/F-SEP	Solvent casting	81.27	30	Drug delivery and wound dressings	Present work

5.12 AgSD Release Kinetics

It is evident from the regression coefficients from the Figures (4.22 - 4.25), that drug release data best fitted to Korsmeyer-Peppas model (R^2 0.978). For that reason, it is only discussed in this section. The numerical value of slope "n" is 0.415 which is in accordance to the $n < 0.5$ which means Fickian diffusion process is involved in AgSD release from F-SEP cross-linked CS/PEG hydrogels [152]. For that reason, AgSD release from the reported hydrogels is governed by both diffusion and swelling. The swelling is imparted by the polymeric chain relaxations in aqueous media. Moreover, the AgSD diffusion from hydrogel surface increased because of higher hydrophilic nature of hydrogel during the release process of hydrophobic drug. Consequently, the resistance to AgSD transport in hydrogel lessened. This is in the strong agreement to the previously reported AgSD release studies [153–155]. In conclusion, AgSD release from afore-mentioned CS-based gels obeyed Fickian release mechanism. Initially, the drug is released due to the swelling which is relatively faster. Later on, AgSD concentration gradient regulated drug release governed by the diffusion process.

Chapter 6

Conclusion and Future Work

In present work, F-SEP incorporated CS/PEG hydrogels are successfully prepared by using solvent casting method. SEP functionalization is confirmed by the FTIR. Moreover, development of siloxane associations and interactions of F-SEP clay with polymeric matrix are established. Developments of interactive forces are directly governed by F-SEP amount which is inferred from TG analysis. In addition, hydrogels are highly biodegradable in proteinase-K solution governed by dissolution process. XRD endorsed fabrication of non-crystalline and uniform nature of hydrogel. SEM examination certified effective blending and successful AgSD loading in DSAR-15.

The swelling capabilities of the synthesized hydrogels in distilled water are increased by the increase in F-SEP from 5-20 mg. Water transport in hydrogels is obeyed by non-Fickian diffusion process ($n > 0.5 < 1$). The maximum swelling responses in distilled water are calculated for SAR-20 (2594%). In addition, hydrogels demonstrated pH sensitive swelling and the excellent swelling volumes are observed at pH 2 and 7. Hydrogels reflected higher swelling responses in non-buffer solution as compared to the buffer solution which is attributed to the greater ionic concentration.

Except SAR(cont), each hydrogel formulation displayed EE% > 75%. Therefore, F-SEP directly affected the EE%. Antibacterial action of F-SEP integrated CS/PEG hydrogels is directly influenced by F-SEP amount and SAR-20 revealed

15 mm ± 0.3 of Iz against *E. coli*. On the other hand, SAR-15 sample revealed excellent cell viability (169.84% ± 2.02) against HEK-293 cells. DSAR-15 exhibited 81.27% of AgSD release in PBS solution in 30 hours which is in accordance to the US pharmacopeia standards. The sustained release of AgSD from gel matrix is superior to numerous studies reported in the literature. The release of AgSD from DSAR-15 reflected best fit to Korsmeyer-Peppas model. Moreover, the drug release from hydrogel is in accordance with $n < 0.5$ which means Fickian process is observed for AgSD release from F-SEP reinforced CS/PEG hydrogel. Kinetic data confirmed that swelling and diffusion both are accountable for AgSD release. The reported CS/PEG/F-SEP hydrogels could be exploited for development of antimicrobial drug delivery platforms and wound dressings in modern biomedical engineering after laborious in-vivo testing.

6.1 Future Perspectives

The present work provided a deep insight of CS/PEG/F-SEP hydrogels for delivery of AgSD. However, further exploration is imperative to use them in variety of fields to understand their therapeutic potential.

Evaluation of mechanical properties: Testing mechanical features of CS/PEG/F-SEP hydrogels is very important in order to use them as wound patch and scaffolds for biomedical applications.

Determination of antifungal activity: CS is natural antifungal material. In this study, antibacterial activities of F-SEP reinforced CS/PEG hydrogels are assessed. However, it is anticipated that the fabricated hydrogels may also be antifungal which needs to be inspected experimentally.

Drug delivery platform: F-SEP cross-linked CS/PEG hydrogels can also offer an indigenous, non-toxic, cost effective and biocompatible platform for slow and targeted release of therapeutic drugs by loading some other drugs with poor bioavailability and therapeutic indexes.

Environmental applications: CS/PEG/F-SEP hydrogels could be exploited for removal toxic dyes and heavy metals from water matrices.

Agronomic applications: The reported hydrogels can be useful for controlled fertilizer release, delivery of micronutrients for crops, enhancement of water retention and water holding capacities of soils.

6.2 Recommendations

The present thesis describes the synthesis and characterization of pH sensitive hydrogels comprised of F-SEP, CS and PEG for drug delivery and wound dressing applications. Current work could be further extended by in-vivo investigations, clinical trials for drug release. Moreover, rheological analyses and determination of Shore A hardness is imperative to exploit them for a practical wound dressing material.

Bibliography

[1] H. Wen, H. Jung, and X. Li, "Drug delivery approaches in addressing clinical pharmacology-related issues: opportunities and challenges," *The AAPS Journal*, vol. 17, pp. 1327–1340, 2015.

[2] D. Church, S. Elsayed, O. Reid, B. Winston, and R. Lindsay, "Burn wound infections," *Clinical Microbiology Reviews*, vol. 19, pp. 403–434, 2006.

[3] H. Soedjana, J. Nadia, A. Sundoro, L. Hasibuan, I. Rubianti, A. Putri, R. Septrina, B. Riestiano, A. T. Prasetyo, and S. Harianti, "The profile of severe burn injury patients with sepsis in hasan sadikin bandung general hospital," *Annals of Burns and Fire Disasters*, vol. 33, p. 312, 2020.

[4] M. M. Al-Rajabi and Y. H. Teow, "Temperature-responsive hydrogel for silver sulfadiazine drug delivery: optimized design and in vitro/in vivo evaluation," *Gels*, vol. 9, p. 329, 2023.

[5] H. Razavi, M. H. Darvishi, and S. Janfaza, "Silver sulfadiazine encapsulated in lipid-based nanocarriers for burn treatment," *Journal of Burn Care & Research*, vol. 39, pp. 319–325, 2018.

[6] E. M. Ahmed, F. S. Aggor, A. M. Awad, and A. T. El-Aref, "An innovative method for preparation of nanometal hydroxide superabsorbent hydrogel," *Carbohydrate Polymers*, vol. 91, pp. 693–698, Jan 16 2013.

[7] L. Gasperini, J. F. Mano, and R. L. Reis, "Natural polymers for the microencapsulation of cells," *Journal of the Royal Society Interface*, vol. 11, p. 20140817, Nov 6 2014.

[8] S. K. Gulrez, S. Al-Assaf, and G. O. Phillips, *Hydrogels: methods of preparation, characterisation and applications*, 2011, pp. 117–150.

[9] M. A. Matica, F. L. Aachmann, A. Tøndervik, H. Sletta, and V. Ostafe, "Chitosan as a wound dressing starting material: Antimicrobial properties and mode of action," *International Journal of Molecular Sciences*, vol. 20, p. 5889, 2019.

[10] J. Zhao, P. Qiu, Y. Wang, Y. Wang, J. Zhou, B. Zhang, L. Zhang, and D. Gou, "Chitosan-based hydrogel wound dressing: From mechanism to applications, a review," *International Journal of Biological Macromolecules*, vol. 244, p. 125250, 2023.

[11] H. Liu, C. Wang, C. Li, Y. Qin, Z. Wang, F. Yang, Z. Li, and J. Wang, "A functional chitosan-based hydrogel as a wound dressing and drug delivery system in the treatment of wound healing," *RSC Advances*, vol. 8, pp. 7533–7549, 2018.

[12] T. C. Ho, C. C. Chang, H. P. Chan, T. W. Chung, C. W. Shu, K. P. Chuang, T. H. Duh, M. H. Yang, and Y. C. Tyan, "Hydrogels: Properties and applications in biomedicine," *Molecules*, vol. 27, May 2 2022.

[13] M. Bahram, N. Mohseni, and M. Moghtader, *An introduction to hydrogels and some recent applications*. IntechOpen, 2016.

[14] B. Wang, H. Xiao, G. Tao, W. Guo, L. Li, H. Wang, J. Su, Z. Zheng, D. Zhou, and L. Chen, "In situ lanthanum growth in magnetic chitosan microgel for accelerated phosphate separation from water: Metal efficiency, specific hydrogel swelling, and mechanistic insights," *ACS ES&T Water*, vol. 5, pp. 1426–1436, 2025.

[15] A. Rasool and A. Islam, *Hydrogels and Their Emerging Applications*, 2023.

[16] M. A. U. R. Qureshi, N. Arshad, A. Rasool, A. Islam, M. Rizwan, M. Haseeb, T. Rasheed, and M. Bilal, "Chitosan and carrageenan-based biocompatible hydrogel platforms for cosmeceutical, drug delivery, and biomedical applications," *Starch-Stärke*, vol. 76, p. 2200052, 2024.

[17] S. Garg, A. Garg, and R. Vishwavidyalaya, "Hydrogel: Classification, properties, preparation and technical features," *Asian Journal of Biomaterial Research*, vol. 2, pp. 163–170, 2016.

[18] G. R. Deen and X. J. Loh, "Stimuli-responsive cationic hydrogels in drug delivery applications," *Gels*, vol. 4, p. 13, 2018.

[19] Z. Yang, D. J. McClements, C. Li, S. Sang, L. Chen, J. Long, C. Qiu, and Z. Jin, "Targeted delivery of hydrogels in human gastrointestinal tract: A review," *Food Hydrocolloids*, vol. 134, p. 108013, 2023.

[20] M. Rizwan, R. Yahya, A. Hassan, M. Yar, A. D. Azzahari, V. Selvanathan, F. Sonsudin, and C. N. Abouloula, "ph sensitive hydrogels in drug delivery: Brief history, properties, swelling, and release mechanism, material selection and applications," *Polymers*, vol. 9, p. 137, 2017.

[21] A. C. Kumar and H. Erothu, *Synthetic polymer hydrogels*, 2016, pp. 141–162.

[22] D. Schmaljohann, "Thermo-and ph-responsive polymers in drug delivery," *Advanced Drug Delivery Reviews*, vol. 58, pp. 1655–1670, 2006.

[23] M. Grassi, G. Grassi, R. Lapasin, and I. Colombo, *Understanding Drug Release and Absorption Mechanisms: A Physical and Mathematical Approach*. CRC Press, 2006.

[24] A. Rakoff, L. G. Feo, and L. Goldstein, "The biologic characteristics of the normal vagina," *American Journal of Obstetrics and Gynecology*, vol. 47, pp. 467–494, 1944.

[25] Y. Zhang, Z. Liu, S. Swaddiwudhipong, H. Miao, Z. Ding, and Z. Yang, "ph-sensitive hydrogel for micro-fluidic valve," *Journal of Functional Biomaterials*, vol. 3, pp. 464–479, 2012.

[26] S. Baliga, S. Muglikar, and R. Kale, "Salivary ph: A diagnostic biomarker," *Journal of Indian Society of Periodontology*, vol. 17, p. 461, 2013.

[27] S. Bashir, M. Hina, J. Iqbal, A. H. Rajpar, M. A. Mujtaba, N. A. Alghamdi, S. Wageh, K. Ramesh, and S. Ramesh, "Fundamental concepts of hydrogels:

Synthesis, properties, and their applications," *Polymers*, vol. 12, Nov 16 2020.

[28] D. Nanda, D. Behera, S. S. Pattnaik, and A. K. Behera, "Advances in natural polymer-based hydrogels: synthesis, applications, and future directions in biomedical and environmental fields," *Discover Polymers*, vol. 2, p. 6, 2025.

[29] M. K. Azeem, A. Islam, R. U. Khan, A. Rasool, M. A. u. R. Qureshi, M. Rizwan, F. Sher, and T. Rasheed, "Eco-friendly three-dimensional hydrogels for sustainable agricultural applications: Current and future scenarios," *Polymers for Advanced Technologies*, 2023.

[30] M. Petchsangsai, W. Sajomsang, P. Gonil, O. Nuchuchua, B. Sutapun, S. Puttipipatkhachorn, and U. R. Ruktanonchai, "A water-soluble methylated n-(4-n, n-dimethylaminocinnamyl) chitosan chloride as novel mucoadhesive polymeric nanocomplex platform for sustained-release drug delivery," *Carbohydrate Polymers*, vol. 83, pp. 1263–1273, 2011.

[31] D. Depan, A. P. Kumar, and R. P. Singh, "Cell proliferation and controlled drug release studies of nanohybrids based on chitosan-g-lactic acid and montmorillonite," *Acta Biomaterialia*, vol. 5, pp. 93–100, 2009.

[32] S. Jabeen, A. Islam, A. Ghaffar, N. Gull, A. Hameed, A. Bashir, T. Jamil, and T. Hussain, "Development of a novel ph sensitive silane crosslinked injectable hydrogel for controlled release of neomycin sulfate," *International Journal of Biological Macromolecules*, vol. 97, pp. 218–227, 2017.

[33] A. Islam, T. Yasin, I. Bano, and M. Riaz, "Controlled release of aspirin from ph-sensitive chitosan/poly (vinyl alcohol) hydrogel," *Journal of Applied Polymer Science*, vol. 124, pp. 4184–4192, 2012.

[34] A. Rasool, M. Rizwan, A. Islam, H. Abdullah, S. S. Shafqat, M. K. Azeem, T. Rasheed, and M. Bilal, "Chitosan-based smart polymeric hydrogels and their prospective applications in biomedicine," *Starch-Stärke*, vol. 76, p. 2100150, 2024.

[35] M. A. F. Monteiro, B. Faria, I. C. F. Moraes, and L. Hilliou, "Hybrid carrageenans versus kappa–iota-carrageenan blends: a comparative study of hydrogel elastic properties," *Gels*, vol. 11, p. 157, 2025.

[36] M. Abbasi, M. Sohail, M. U. Minhas, S. Khan, Z. Hussain, A. Mahmood, S. A. Shah, and M. Kousar, "Novel biodegradable ph-sensitive hydrogels: An efficient controlled release system to manage ulcerative colitis," *International Journal of Biological Macromolecules*, vol. 136, pp. 83–96, Sep 1 2019.

[37] U. S. Madduma-Bandarage and S. V. Madihally, "Synthetic hydrogels: Synthesis, novel trends, and applications," *Journal of Applied Polymer Science*, vol. 138, p. 50376, 2021.

[38] M. Endres, D. Hutmacher, A. Salgado, C. Kaps, J. Ringe, R. Reis, M. Sittinger, A. Brandwood, and J.-T. Schantz, "Osteogenic induction of human bone marrow-derived mesenchymal progenitor cells in novel synthetic polymer–hydrogel matrices," *Tissue Engineering*, vol. 9, pp. 689–702, 2003.

[39] Q. Wei, N.-N. Deng, J. Guo, and J. Deng, "Synthetic polymers for biomedical applications," *International Journal of Biomaterials*, vol. 2018, p. 7158621, 2018.

[40] Z. Hussain, H. E. Thu, A. N. Shuid, H. Katas, and F. Hussain, "Recent advances in polymer-based wound dressings for the treatment of diabetic foot ulcer: an overview of state-of-the-art," *Current Drug Targets*, vol. 19, pp. 527–550, 2018.

[41] N. A. Peppas, K. B. Keys, M. Torres-Lugo, and A. M. Lowman, "Poly (ethylene glycol)-containing hydrogels in drug delivery," *Journal of Controlled Release*, vol. 62, pp. 81–87, 1999.

[42] S. Sun, Y. Cui, B. Yuan, M. Dou, G. Wang, H. Xu, J. Wang, W. Yin, D. Wu, and C. Peng, "Drug delivery systems based on polyethylene glycol hydrogels for enhanced bone regeneration," *Frontiers in Bioengineering and Biotechnology*, vol. 11, p. 1117647, 2023.

[43] C. J. G. Abrego, L. Dedroog, O. Deschaume, J. Wellens, A. Vananroye, M. P. Lettinga, J. Patterson, and C. Bartic, "Multiscale characterization of the mechanical properties of fibrin and polyethylene glycol (peg) hydrogels for tissue engineering applications," *Macromolecular Chemistry and Physics*, vol. 223, p. 2100366, 2022.

[44] A. Mahardian, "Biocompatible hydrogel film of polyethylene oxide-polyethylene glycol dimetacrylate for wound dressing application," in *IOP Conference Series: Materials Science and Engineering*, 2018, p. 012076.

[45] A. A. D'souza and R. Shegokar, "Polyethylene glycol (peg): a versatile polymer for pharmaceutical applications," *Expert Opinion on Drug Delivery*, vol. 13, pp. 1257–1275, 2016.

[46] A. Rasool, S. Ata, A. Islam, M. Rizwan, M. K. Azeem, A. Mehmood, R. U. Khan, and H. A. Mahmood, "Kinetics and controlled release of lidocaine from novel carrageenan and alginate-based blend hydrogels," *International Journal of Biological Macromolecules*, vol. 147, pp. 67–78, 2020.

[47] F. Song, X. Li, Q. Wang, L. Liao, and C. Zhang, "Nanocomposite hydrogels and their applications in drug delivery and tissue engineering," *Journal of Biomedical Nanotechnology*, vol. 11, pp. 40–52, 2015.

[48] J. Yi, G. Choe, J. Park, and J. Y. Lee, "Graphene oxide-incorporated hydrogels for biomedical applications," *Polymer Journal*, vol. 52, pp. 823–837, 2020.

[49] A. Vicosa, A. Gomes, B. Soares, and C. Paranhos, "Effect of sepiolite on the physical properties and swelling behavior of rifampicin-loaded nanocomposite hydrogels," *Express Polymer Letters*, vol. 3, pp. 518–524, 2009.

[50] L. Alves, E. Ferraz, J. Santarén, M. G. Rasteiro, and J. A. Gamelas, "Improving colloidal stability of sepiolite suspensions: Effect of the mechanical disperser and chemical dispersant," *Minerals*, vol. 10, p. 779, 2020.

[51] F. N. Shamsabad, M. H. Salehi, J. Shams, and T. Ghazanfari, "Cytotoxicity of bentonite, zeolite, and sepiolite clay minerals on peripheral blood mononuclear cells," *Immunoregulation*, vol. 5, pp. 121–130, 2023.

[52] X. Zhang, H. Guo, N. Xiao, X. Ma, C. Liu, L. Zhong, and G. Xiao, "Preparation and properties of epichlorohydrin-cross-linked chitosan/hydroxyethyl cellulose based cuo nanocomposite films," *Cellulose*, vol. 29, pp. 4413–4426, 2022.

[53] N. A. Peppas and B. D. Barr-Howell, *Characterization of the cross-linked structure of hydrogels*. CRC Press, 2019, pp. 27–56.

[54] Y. Xia, Z. Ma, X. Wu, H. Wei, H. Zhang, G. Li, Y. Qian, M. Shahriari-Khalaji, K. Hou, and R. Cao, "Advances in stimuli-responsive chitosan hydrogels for drug delivery systems," *Macromolecular Bioscience*, vol. 24, p. 2300399, 2024.

[55] A. Kausar, "Scientific potential of chitosan blending with different polymeric materials: A review," *Journal of Plastic Film & Sheeting*, vol. 33, pp. 384–412, 2017.

[56] T. S. Daitx, M. Giovanela, L. N. Carli, and R. S. Mauler, "Biodegradable polymer/clay systems for highly controlled release of npk fertilizer," *Polymers for Advanced Technologies*, vol. 30, pp. 631–639, 2019.

[57] A. Rasool, M. Rizwan, T. Rasheed, and M. Bilal, *Thermo-responsive functionalized polymeric nanocomposites*. Elsevier, 2023, pp. 219–240.

[58] A. Rasool, S. Ata, and A. Islam, "Stimuli responsive biopolymer (chitosan) based blend hydrogels for wound healing application," *Carbohydrate Polymers*, vol. 203, pp. 423–429, 2019.

[59] M. A. u. R. Qureshi, N. Arshad, A. Rasool, M. Rizwan, and T. Rasheed, "Graphene oxide reinforced biopolymeric (chitosan) hydrogels for controlled cephradine release," *International Journal of Biological Macromolecules*, vol. 242, p. 124948, Jul 1 2023.

[60] M. A. U. R. Qureshi, N. Arshad, A. Rasool, M. Rizwan, K. F. Fawy, and T. Rasheed, "ph-responsive chitosan dendrimer hydrogels enabling controlled cefixime release," *European Polymer Journal*, vol. 219, p. 113377, 2024.

[61] M. Naz, M. Rizwan, S. Jabeen, A. Ghaffar, A. Islam, N. Gull, A. Rasool, R. U. Khan, S. Z. Alshawwa, and M. Iqbal, "Cephradine drug release using electrospun chitosan nanofibers incorporated with halloysite nanoclay," *Zeitschrift für Physikalische Chemie*, vol. 236, pp. 227–238, 2022.

[62] F. N. Sorasitthiyanukarn, C. Muangnoi, P. R. N. Bhuket, P. Rojsitthisak, and P. Rojsitthisak, "Chitosan/alginate nanoparticles as a promising approach for oral delivery of curcumin diglutaric acid for cancer treatment," *Materials Science and Engineering: C*, vol. 93, pp. 178–190, 2018.

[63] A. Lejardi, R. Hernández, M. Criado, J. I. Santos, A. Etxeberria, J. Sarasua, and C. Mijangos, "Novel hydrogels of chitosan and poly(vinyl alcohol)-g-glycolic acid copolymer with enhanced rheological properties," *Carbohydrate Polymers*, vol. 103, pp. 267–273, 2014.

[64] L. G. Gómez-Mascaraque, J. A. Méndez, M. Fernández-Gutiérrez, B. Vázquez, and J. S. Román, "Oxidized dextrins as alternative crosslinking agents for polysaccharides: application to hydrogels of agarose–chitosan," *Acta Biomaterialia*, vol. 10, pp. 798–811, 2014.

[65] L. Zhang, L. Wang, B. Guo, and P. X. Ma, "Cytocompatible injectable carboxymethyl chitosan/n-isopropylacrylamide hydrogels for localized drug delivery," *Carbohydrate Polymers*, vol. 103, pp. 110–118, 2014.

[66] A. Islam and T. Yasin, "Controlled delivery of drug from ph sensitive chitosan/poly(vinyl alcohol) blend," *Carbohydrate Polymers*, vol. 88, pp. 1055–1060, 2012.

[67] F. Liu, B. Qin, L. He, and R. Song, "Novel starch/chitosan blending membrane: Antibacterial, permeable and mechanical properties," *Carbohydrate Polymers*, vol. 78, pp. 146–150, 2009.

[68] D. Archana, J. Dutta, and P. Dutta, "Evaluation of chitosan nano dressing for wound healing: Characterization, in vitro and in vivo studies," *International Journal of Biological Macromolecules*, vol. 57, pp. 193–203, 2013.

[69] A. M. Mazen, D. E. M. Radwan, and A. F. Ahmed, "Growth responses of maize plants cultivated in sandy soil amended by different superabsorbant hydrogels," *Journal of Plant Nutrition*, vol. 38, pp. 325–337, 2015.

[70] B. V. Slaughter, S. S. Khurshid, O. Z. Fisher, A. Khademhosseini, and N. A. Peppas, "Hydrogels in regenerative medicine," *Advanced Materials*, vol. 21, pp. 3307–3329, 2009.

[71] R. Rajakumar and J. Sankar, "Hydrogel: Novel soil conditioner and safer delivery vehicle for fertilizers and agrochemicals–a review," *International Journal of Applied and Pure Science and Agriculture*, vol. 2, pp. 163–172, 2016.

[72] D.-M. Radulescu, I. A. Neacsu, A.-M. Grumezescu, and E. Andronescu, "New insights of scaffolds based on hydrogels in tissue engineering," *Polymers*, vol. 14, p. 799, 2022.

[73] P. Gupta, K. Vermani, and S. Garg, "Hydrogels: from controlled release to ph-responsive drug delivery," *Drug Discovery Today*, vol. 7, pp. 569–579, 2002.

[74] N. Graham, G. NB, and W. DA, "Hydrogels and biodegradable polymers for the controlled delivery of drugs," 1982.

[75] K. d. Yao, T. Peng, M. x. Xu, C. Yuan, M. F. Goosen, Q. q. Zhang, and L. Ren, "ph-dependent hydrolysis and drug release of chitosan/polyether interpenetrating polymer network hydrogel," *Polymer International*, vol. 34, pp. 213–219, 1994.

[76] T. K. Giri, A. Thakur, A. Alexander, H. Badwaik, and D. K. Tripathi, "Modified chitosan hydrogels as drug delivery and tissue engineering systems: present status and applications," *Acta Pharmaceutica Sinica B*, vol. 2, pp. 439–449, 2012.

[77] J. Ahn, J. Ryu, G. Song, M. Whang, and J. Kim, "Network structure and enzymatic degradation of chitosan hydrogels determined by crosslinking methods," *Carbohydrate Polymers*, vol. 217, pp. 160–167, 2019.

[78] L. Wang, H. Lv, L. Liu, Q. Zhang, P. Nakielski, Y. Si, J. Cao, X. Li, F. Pierini, and J. Yu, "Electrospun nanofiber-reinforced three-dimensional chitosan matrices: Architectural, mechanical and biological properties," *Journal of Colloid and Interface Science*, vol. 565, pp. 416–425, 2020.

[79] A. N. A. U. R. Q. M, R. A, J. NK, B. MS, N. U. R. Q. M, and I. H, "Kappa-carrageenan and sodium alginate-based ph-responsive hydrogels for controlled release of methotrexate," *Royal Society Open Science*, p. 231952, Apr 24 2024.

[80] M. A. J. Shaikh, G. Gupta, O. Afzal, M. M. Gupta, A. Goyal, A. S. A. Altamimi, S. I. Alzarea, W. H. Almalki, I. Kazmi, and P. Negi, "Sodium alginate-based drug delivery for diabetes management: A review," *International Journal of Biological Macromolecules*, vol. 236, p. 123986, 2023.

[81] N. Mor and N. Raghav, "In-vitro simulation of modified-alginate ester as sustained release delivery system for curcumin," *Journal of Molecular Structure*, vol. 1283, p. 135307, 2023.

[82] A. Sosnik, "Alginate particles as platform for drug delivery by the oral route: state-of-the-art," *International Scholarly Research Notices*, vol. 2014, p. 926157, 2014.

[83] K. Zhang, X. Luo, L. Yang, Z. Chang, and S. Luo, "Progress toward hydrogels in removing heavy metals from water: Problems and solutions—a review," *ACS ES&T Water*, vol. 1, pp. 1098–1116, 2021.

[84] M. Chelu, A. M. Musuc, M. Popa, and J. M. C. Moreno, "Chitosan hydrogels for water purification applications," *Gels*, vol. 9, p. 664, 2023.

[85] T. Velnar, T. Bailey, and V. Smrkolj, "The wound healing process: an overview of the cellular and molecular mechanisms," *Journal of International Medical Research*, vol. 37, pp. 1528–1542, 2009.

[86] H. N. Wilkinson and M. J. Hardman, "Wound healing: cellular mechanisms and pathological outcomes," *Open Biology*, vol. 10, p. 200223, 2020.

[87] M. Kloc, R. M. Ghobrial, J. Wosik, A. Lewicka, S. Lewicki, and J. Z. Kubiak, "Macrophage functions in wound healing," *Journal of Tissue Engineering and Regenerative Medicine*, vol. 13, pp. 99–109, 2019.

[88] W. Guo, X. Ding, H. Zhang, Z. Liu, Y. Han, Q. Wei, O. V. Okoro, A. Shavandi, and L. Nie, "Recent advances of chitosan-based hydrogels for skin-wound dressings," *Gels*, vol. 10, p. 175, 2024.

[89] R. C. Goy, D. d. Britto, and O. B. Assis, "A review of the antimicrobial activity of chitosan," *Polímeros*, vol. 19, pp. 241–247, 2009.

[90] C. Yang, Y. Chen, H. Huang, S. Fan, C. Yang, L. Wang, W. Li, W. Niu, and J. Liao, "Ros-eliminating carboxymethyl chitosan hydrogel to enhance burn wound-healing efficacy," *Frontiers in Pharmacology*, vol. 12, p. 679580, 2021.

[91] H. Geng, P. Zhang, L. Liu, Y. Shangguan, X. Cheng, H. Liu, Y. Zhao, J. Hao, W. Li, and J. Cui, "Convergent architecting of multifunction-in-one hydrogels as wound dressings for surgical anti-infections," *Materials Today Chemistry*, vol. 25, p. 100968, 2022.

[92] Z. Tan, X. Li, C. Yu, M. Yao, Z. Zhao, B. Guo, L. Liang, Y. Wei, F. Yao, and H. Zhang, "A self-gelling powder based on polyacrylic acid/polyacrylamide/quaternate chitosan for rapid hemostasis," *International Journal of Biological Macromolecules*, vol. 232, p. 123449, 2023.

[93] Q. Bai, Q. Gao, F. Hu, C. Zheng, W. Chen, N. Sun, J. Liu, Y. Zhang, X. Wu, and T. Lu, "Chitosan and hyaluronic-based hydrogels could promote the infected wound healing," *International Journal of Biological Macromolecules*, vol. 232, p. 123271, 2023.

[94] J. L. Soriano-Ruiz, A. C. Calpena-Campmany, M. Silva-Abreu, L. Halbout-Bellowa, N. B. de Febrer, M. J. Rodriguez-Lagunas, and B. Clares-Naveros,

"Design and evaluation of a multifunctional thermosensitive poloxamer-chitosan-hyaluronic acid gel for the treatment of skin burns," *International Journal of Biological Macromolecules*, vol. 142, pp. 412–422, 2020.

[95] A. Kirichenko, I. Bolshakov, A. Ali-Rizal, and A. Vlasov, "Morphological study of burn wound healing with the use of collagen-chitosan wound dressing," *Bulletin of Experimental Biology and Medicine*, vol. 154, pp. 692–696, 2013.

[96] S. Aoyagi, H. Onishi, and Y. Machida, "Novel chitosan wound dressing loaded with minocycline for the treatment of severe burn wounds," *International Journal of Pharmaceutics*, vol. 330, pp. 138–145, 2007.

[97] T. Wang, X.-K. Zhu, X.-T. Xue, and D.-Y. Wu, "Hydrogel sheets of chitosan, honey and gelatin as burn wound dressings," *Carbohydrate Polymers*, vol. 88, pp. 75–83, 2012.

[98] C.-M. Deng, L.-Z. He, M. Zhao, D. Yang, and Y. Liu, "Biological properties of the chitosan-gelatin sponge wound dressing," *Carbohydrate Polymers*, vol. 69, pp. 583–589, 2007.

[99] O. M. Dragostin, S. K. Samal, M. Dash, F. Lupascu, A. Pânzariu, C. Tuchilus, N. Ghetu, M. Danciu, P. Dubruel, and D. Pieptu, "New antimicrobial chitosan derivatives for wound dressing applications," *Carbohydrate Polymers*, vol. 141, pp. 28–40, 2016.

[100] S. Alven and B. A. Aderibigbe, "Chitosan-based scaffolds incorporated with silver nanoparticles for the treatment of infected wounds," *Pharmaceutics*, vol. 16, p. 327, 2024.

[101] H. Wu, L. Zhu, L. Xie, T. Zhou, T. Yu, and Y. Zhang, "A chitosan-based light-curing hydrogel dressing for accelerated healing of infected wounds," *International Journal of Biological Macromolecules*, vol. 278, p. 134609, 2024.

[102] V. Pawar, M. Dhanka, and R. Srivastava, "Cefuroxime conjugated chitosan hydrogel for treatment of wound infections," *Colloids and Surfaces B: Biointerfaces*, vol. 173, pp. 776–787, 2019.

[103] H. Liu, R. Chen, P. Wang, J. Fu, Z. Tang, J. Xie, Y. Ning, J. Gao, Q. Zhong, and X. Pan, "Electrospun polyvinyl alcohol-chitosan dressing stimulates infected diabetic wound healing with combined reactive oxygen species scavenging and antibacterial abilities," *Carbohydrate Polymers*, vol. 316, p. 121050, 2023.

[104] M. Burkatovskaya, A. P. Castano, T. N. Demidova-Rice, G. P. Tegos, and M. R. Hamblin, "Effect of chitosan acetate bandage on wound healing in infected and noninfected wounds in mice," *Wound Repair and Regeneration*, vol. 16, pp. 425–431, 2008.

[105] P. Chidchai, K. Singpanna, P. Opanasopit, P. Patrojanasophon, and C. Pornpitchanarong, "Development of photo-crosslinked chitosan-methacrylate hydrogel incorporated with ciprofloxacin as dressing for infected wounds," *Carbohydrate Polymer Technologies and Applications*, vol. 7, p. 100478, 2024.

[106] X. Wei, C. Liu, Z. Li, Z. Gu, J. Yang, and K. Luo, "Chitosan-based hydrogel dressings for diabetic wound healing via promoting m2 macrophage-polarization," *Carbohydrate Polymers*, vol. 331, p. 121873, 2024.

[107] S. A. Majd, M. R. Khorasgani, S. J. Moshtaghian, A. Talebi, and M. Khezri, "Application of chitosan/pva nano fiber as a potential wound dressing for streptozotocin-induced diabetic rats," *International Journal of Biological Macromolecules*, vol. 92, pp. 1162–1168, 2016.

[108] L. Colobatiu, A. Gavan, A.-V. Potarniche, V. Rus, Z. Diaconeasa, A. Mocan, I. Tomuta, S. Mirel, and M. Mihaiu, "Evaluation of bioactive compounds-loaded chitosan films as a novel and potential diabetic wound dressing material," *Reactive and Functional Polymers*, vol. 145, p. 104369, 2019.

[109] B.-Y. Lim, F. Azmi, and S.-F. Ng, "Ll37 microspheres loaded on activated carbon-chitosan hydrogel: Anti-bacterial and anti-toxin wound dressing for chronic wound infections," *AAPS PharmSciTech*, vol. 25, p. 110, 2024.

[110] S. Shahroudi, A. Parvinnasab, E. Salahinejad, S. Abdi, S. Rajabi, and L. Tayebi, "Efficacy of 3d-printed chitosan-cerium oxide dressings coated with vancomycin for chronic wounds management," *Carbohydrate Polymers*, vol. 349, p. 123036, 2025.

[111] F. V. Borbolla-Jiménez, S. I. Peña-Corona, S. J. Farah, M. T. Jiménez-Valdés, E. Pineda-Pérez, A. Romero-Montero, M. L. Del Prado-Audelo, S. A. Bernal-Chávez, J. J. Magaña, and G. Leyva-Gómez, "Films for wound healing fabricated using a solvent casting technique," *Pharmaceutics*, vol. 15, p. 1914, 2023.

[112] S. Kazarian and K. Chan, "Applications of atr-ftir spectroscopic imaging to biomedical samples," *Biochimica et Biophysica Acta - Biomembranes*, vol. 1758, pp. 858–867, 2006.

[113] R. B. Prime, H. E. Bair, S. Vyazovkin, P. K. Gallagher, and A. Riga, "Thermogravimetric analysis (tga)," in *Thermal Analysis of Polymers: Fundamentals and Applications*, 2009, pp. 241–317.

[114] C. G. Pope, "X-ray diffraction and the bragg equation," *Journal of Chemical Education*, vol. 74, p. 129, 1997.

[115] A. S. Panwar, A. Singh, and S. Sehgal, "Material characterization techniques in engineering applications: A review," *Materials Today: Proceedings*, vol. 28, pp. 1932–1937, 2020.

[116] S. Colombi, L. P. Macor, L. Ortiz-Membrado, S. Pérez-Amodio, E. Jiménez-Piqué, E. Engel, M. M. Pérez-Madrigal, J. García-Torres, and C. Alemán, "Enzymatic degradation of polylactic acid fibers supported on a hydrogel for sustained release of lactate," *ACS Applied Bio Materials*, vol. 6, pp. 3889–3901, 2023.

[117] M. A. U. R. Qureshi, N. Arshad, A. Rasool, M. Rizwan, and T. Rasheed, "Guar gum-based stimuli responsive hydrogels for sustained release of diclofenac sodium," *International Journal of Biological Macromolecules*, vol. 250, p. 126275, 2023.

[118] M. N. U. R. Qureshi, M. Qayyum, A. Riaz, M. A. U. R. Qureshi, A. Rasool, and M. Kanwal, "Cultivation, identification, and parameter optimization of chicken embryo fibroblast (cef) in primary culture," *Scientific Inquiry and Review*, vol. 8, pp. 64–88, 2024.

[119] H. Manzoor, N. Arshad, M. A. U. R. Qureshi, and A. Javed, "Hydroxyapatite-reinforced pectin hydrogel films pec/pva/aptes/hap: doxycycline loading for sustained drug release and wound healing applications," *RSC Advances*, vol. 15, pp. 30 026–30 045, 2025.

[120] A. Rasool, S. Ata, A. Islam, and R. U. Khan, "Fabrication of novel carrageenan based stimuli responsive injectable hydrogels for controlled release of cephradine," *RSC Advances*, vol. 9, pp. 12 282–12 290, 2019.

[121] N. Gull, S. M. Khan, O. M. Butt, A. Islam, A. Shah, S. Jabeen, S. U. Khan, A. Khan, R. U. Khan, and M. T. Z. Butt, "Inflammation targeted chitosan-based hydrogel for controlled release of diclofenac sodium," *International Journal of Biological Macromolecules*, vol. 162, pp. 175–187, 2020.

[122] D. G. Kanjickal and S. T. Lopina, "Modeling of drug release from polymeric delivery systems—a review," *Critical Reviews in Therapeutic Drug Carrier Systems*, vol. 21, p. 10343, 2004.

[123] K. Zhang, W. Feng, and C. Jin, "Protocol efficiently measuring the swelling rate of hydrogels," *MethodsX*, vol. 7, p. 100779, 2020.

[124] X. He, J. Li, S. An, and C. Jiang, "ph-sensitive drug-delivery systems for tumor targeting," *Therapeutic Delivery*, vol. 4, pp. 1499–1510, 2013.

[125] S. R. Mane, A. Sathyan, and R. Shunmugam, "Biomedical applications of ph-responsive amphiphilic polymer nanoassemblies," *ACS Applied Nano Materials*, vol. 3, pp. 2104–2117, 2020.

[126] S. Lazarević, I. Janković-Častvan, D. Jovanović, S. Milonjić, D. Janaćković, and R. Petrović, "Adsorption of pb2+, cd2+ and sr2+ ions onto natural and acid-activated sepiolites," *Applied Clay Science*, vol. 37, pp. 47–57, 2007.

[127] M. Naz, S. Jabeen, N. Gull, A. Ghaffar, A. Islam, M. Rizwan, H. Abdullah, A. Rasool, S. Khan, and R. Khan, "Novel silane crosslinked chitosan based electrospun nanofiber for controlled release of benzocaine," *Frontiers in Materials*, vol. 9, p. 826251, 2022.

[128] I. M. Deygen and E. V. Kudryashova, "New versatile approach for analysis of peg content in conjugates and complexes with biomacromolecules based on ftir spectroscopy," *Colloids and Surfaces B: Biointerfaces*, vol. 141, pp. 36–43, 2016.

[129] H. Staroszczyk, K. Sztuka, J. Wolska, A. Wojtasz-Pająk, and I. Kołodziejska, "Interactions of fish gelatin and chitosan in uncrosslinked and crosslinked with edc films: Ft-ir study," *Spectrochimica Acta Part A: Molecular and Biomolecular Spectroscopy*, vol. 117, pp. 707–712, 2014.

[130] P. Z. Hong, S. D. Li, C. Y. Ou, C. P. Li, L. Yang, and C. H. Zhang, "Thermogravimetric analysis of chitosan," *Journal of Applied Polymer Science*, vol. 105, pp. 547–551, 2007.

[131] H. F. Barbosa, D. S. Francisco, A. P. Ferreira, and . T. Cavalheiro, "A new look towards the thermal decomposition of chitins and chitosans with different degrees of deacetylation by coupled tg-ftir," *Carbohydrate Polymers*, vol. 225, p. 115232, 2019.

[132] H. Moussout, H. Ahlafi, M. Aazza, and M. Bourakhouadar, "Kinetics and mechanism of the thermal degradation of biopolymers chitin and chitosan using thermogravimetric analysis," *Polymer Degradation and Stability*, vol. 130, pp. 1–9, 2016.

[133] L. h. He, R. Xue, D. b. Yang, Y. Liu, and R. Song, "Effects of blending chitosan with peg on surface morphology, crystallization and thermal properties," *Chinese Journal of Polymer Science*, vol. 27, pp. 501–510, 2009.

[134] K. Divya, S. Rebello, and M. Jisha, "A simple and effective method for extraction of high purity chitosan from shrimp shell waste," in *Proceedings of the International Conference on Advances in Applied Science and Environmental Engineering-ASEE*, 2014, pp. 141–145.

[135] M. S. D. Río, E. Garcia-Romero, M. Suárez, I. D. Silva, L. Fuentes-Montero, and G. Martínez-Criado, "Variability in sepiolite: Diffraction studies," *American Mineralogist*, vol. 96, pp. 1443–1454, 2011.

[136] Y. Jiang, L. Wang, W. Qi, P. Yin, X. Liao, Y. Luo, and Y. Ding, "Antibacterial and self-healing sepiolite-based hybrid hydrogel for hemostasis and wound healing," *Biomaterials Advances*, vol. 159, p. 213838, 2024.

[137] J. Dutta and N. Devi, "Preparation, optimization, and characterization of chitosan-sepiolite nanocomposite films for wound healing," *International Journal of Biological Macromolecules*, vol. 186, pp. 244–254, 2021.

[138] M. K. Azeem, A. Islam, M. Rizwan, A. Rasool, N. Gul, R. U. Khan, S. M. Khan, and T. Rasheed, "Sustainable and environment friendlier carrageenan-based ph-responsive hydrogels: Swelling behavior and controlled release of fertilizers," *Colloid and Polymer Science*, vol. 301, pp. 209–219, 2023.

[139] J. Ostrowska-Czubenko, M. Gierszewska, and M. Pieróg, "ph-responsive hydrogel membranes based on modified chitosan: water transport and kinetics of swelling," *Journal of Polymer Research*, vol. 22, pp. 1–12, 2015.

[140] A. Pourjavadi and G. R. Mahdavinia, "Superabsorbency, ph-sensitivity and swelling kinetics of partially hydrolyzed chitosan-g-poly(acrylamide) hydrogels," *Turkish Journal of Chemistry*, vol. 30, pp. 595–608, 2006.

[141] E. Ruiz-Hitzky, C. Ruiz-García, F. M. Fernandes, G. L. Dico, L. Lisuzzo, V. Prevot, M. Darder, and P. Aranda, "Sepiolite-hydrogels: synthesis by ultrasound irradiation and their use for the preparation of functional clay-based nanoarchitectured materials," *Frontiers in Chemistry*, vol. 9, p. 733105, 2021.

[142] S. Ata, A. Rasool, A. Islam, I. Bibi, M. Rizwan, M. K. Azeem, and M. Iqbal, "Loading of cefixime to ph sensitive chitosan based hydrogel and investigation of controlled release kinetics," *International Journal of Biological Macromolecules*, vol. 155, pp. 1236–1244, 2020.

[143] M. Muller, M. Hollyoak, Z. Moaveni, T. L. H. Brown, D. Herndon, and J. Heggers, "Retardation of wound healing by silver sulfadiazine is reversed by aloe vera and nystatin," *Burns*, vol. 29, pp. 834–836, 2003.

[144] N. A. Mohamed and M. M. Fahmy, "Synthesis and antimicrobial activity of some novel cross-linked chitosan hydrogels," *International Journal of Molecular Sciences*, vol. 13, pp. 11 194–11 209, 2012.

[145] Y. Zhan, W. Zeng, G. Jiang, Q. Wang, X. Shi, Z. Zhou, H. Deng, and Y. Du, "Construction of lysozyme exfoliated rectorite-based electrospun nanofibrous membranes for bacterial inhibition," *Journal of Applied Polymer Science*, vol. 132, 2015.

[146] Q. L. Feng, J. Wu, G. Q. Chen, F. Cui, T. Kim, and J. Kim, "A mechanistic study of the antibacterial effect of silver ions on escherichia coli and staphylococcus aureus," *Journal of Biomedical Materials Research*, vol. 52, pp. 662–668, 2000.

[147] C. Bergonzi, A. Bianchera, G. Remaggi, M. C. Ossiprandi, R. Bettini, and L. Elviri, "3d printed chitosan/alginate hydrogels for the controlled release of silver sulfadiazine in wound healing applications: design, characterization and antimicrobial activity," *Micromachines*, vol. 14, p. 137, 2023.

[148] S. Chakavala, N. Patel, N. V. Pate, V. Thakkar, K. Patel, and T. Gandhi, "Development and in vivo evaluation of silver sulfadiazine loaded hydrogel consisting polyvinyl alcohol and chitosan for severe burns," *Journal of Pharmacy and Bioallied Sciences*, vol. 4, pp. S54–S56, 2012.

[149] K. S. Jodar, V. M. Balcao, M. V. Chaud, M. Tubino, V. M. Yoshida, J. M. O. Jr, and M. M. Vila, "Development and characterization of a hydrogel containing silver sulfadiazine for antimicrobial topical applications," *Journal of Pharmaceutical Sciences*, vol. 104, pp. 2241–2254, 2015.

[150] G. Yaşayan, "Chitosan films and chitosan/pectin polyelectrolyte complexes encapsulating silver sulfadiazine for wound healing," *İstanbul Journal of Pharmacy*, vol. 50, pp. 238–244, 2020.

[151] A. Pandey, M. Momin, and A. Chando, "Silver sulfadiazine loaded breathable hydrogel sponge for wound healing," *Drug Metabolism and Personalized Therapy*, vol. 35, p. 20200124, 2020.

[152] I. Y. Wu, S. Bala, N. Škalko Basnet, and M. P. D. Cagno, "Interpreting non-linear drug diffusion data: Utilizing korsmeyer-peppas model to study drug release from liposomes," *European Journal of Pharmaceutical Sciences*, vol. 138, p. 105026, 2019.

[153] S. Jangra, S. Devi, V. K. Tomer, V. Chhokar, and S. Duhan, "Improved antimicrobial property and controlled drug release kinetics of silver sulfadiazine loaded ordered mesoporous silica," *Journal of Asian Ceramic Societies*, vol. 4, pp. 282–288, 2016.

[154] L. V. Vaz, V. M. Balcão, J. M. O. Jr, M. Tubino, A. Jozala, V. M. H. Yoshida, and M. M. D. C. Vila, "Development and characterization of a hydrogel containing silver sulfadiazine for antimicrobial topical applications. part ii: Stability, cytotoxicity and silver release patterns," *Brazilian Journal of Pharmaceutical Sciences*, vol. 58, p. e18688, 2022.

[155] D. Alshora, L. Ashri, R. Alfaraj, A. Alhusaini, R. Mohammad, N. Alanaze, M. Ibrahim, M. M. Badran, M. Bekhit, and S. Alsaif, "Formulation and in vivo evaluation of biofilm loaded with silver sulfadiazine for burn healing," *Gels*, vol. 9, p. 855, 2023.